AD_____

Award Number: W81XWH-04-1-0182

TITLE: Regulation of Calcium Fluxes and Apoptosis by BCL-2 Family Proteins in Prostate Cancer Cells

PRINCIPAL INVESTIGATOR: David J. McConkey, Ph.D.

CONTRACTING ORGANIZATION: The University of Texas
M.D. Anderson Cancer Center
Houston, TX 77030

REPORT DATE: February 2005

TYPE OF REPORT: Annual

PREPARED FOR: U.S. Army Medical Research and Materiel Command
Fort Detrick, Maryland 21702-5012

REPORT DOCUMENTATION PAGE

Form Approved
OMB No. 074-0188

1. AGENCY USE ONLY	2. REPORT DATE	3. REPORT TYPE AND DATES COVERED
	February 2005	Annual (12 Jan 2004 - 11 Jan 2005)

4. TITLE AND SUBTITLE
Regulation of Calcium Fluxes and Apoptosis by BCL-2 Family Proteins in Prostate Cancer Cells

5. FUNDING NUMBERS
W81XWH-04-1-0182

6. AUTHOR(S)

David J. McConkey, Ph.D.

7. PERFORMING ORGANIZATION NAME(S) AND ADDRESS(ES)

The University of Texas
M.D. Anderson Cancer Center
Houston, TX 77030

E-Mail: dmcconkey@mdanderson.org

8. PERFORMING ORGANIZATION REPORT NUMBER

9. SPONSORING / MONITORING AGENCY NAME(S) AND ADDRESS(ES)

U.S. Army Medical Research and Materiel Command
Fort Detrick, Maryland 21702-5012

10. SPONSORING / MONITORING AGENCY REPORT NUMBER

11. SUPPLEMENTARY NOTES

12a. DISTRIBUTION / AVAILABILITY STATEMENT
Approved for Public Release; Distribution Unlimited

12b. DISTRIBUTION CODE

13. ABSTRACT (Maximum 200 Words)

Members of the BCL-2 family of cell death regulators play critical roles in the progression of androgen-independent, metastatic prostate cancer. Despite years of research, the molecular mechanisms underlying the effects of these proteins remain unclear. In previous studies we demonstrated that BCL-2 family proteins regulate a crucial step in the apoptotic pathway (cytochrome c release) by regulating endoplasmic reticular and mitochondrial calcium fluxes. In this project we are studying these effects in more detail, focusing on the possibility that the so-called "BH3 only" proteins and Bax directly promote endoplasmic reticular calcium release. To this end, we are (1) Defining the effects of mitochondrial calcium uptake on cytochrome c mobilization and release; (2) Determining the effects of BH3 only members of the BCL-2 family on intracellular calcium fluxes; and (3) Identifying possible direct effects of Bax and Bak on ER calcium fluxes. With this information in hand, we expect that we will be able to define therapeutic strategies that directly target the cell death resistance mechanisms that appear to limit the effects of currently available therapies.

14. SUBJECT TERMS
Cancer Biology, apoptosis, cytochrome c release, BH3 only proteins

15. NUMBER OF PAGES
87

16. PRICE CODE

17. SECURITY CLASSIFICATION OF REPORT	18. SECURITY CLASSIFICATION OF THIS PAGE	19. SECURITY CLASSIFICATION OF ABSTRACT	20. LIMITATION OF ABSTRACT
Unclassified	Unclassified	Unclassified	Unlimited

Table of Contents

INTRODUCTION

Prostate cancer remains the most common malignancy in American men and is the second leading cause of cancer-related death (1). Advances in early detection have led to better surgical control of the disease, but less progress has been made in the treatment of metastatic cancer. Androgen ablation remains the therapy of choice for patients with metastatic prostate cancer, and almost all patients initially benefit from this approach. However, almost all patients ultimately relapse with androgen-independent cancer, and the treatment options for these patients are limited (2).

Investigation into the molecular mechanisms that mediate the effects of androgen ablation has established that apoptosis plays a central role, and defects in the control of apoptosis in androgen-independent tumors not only undermine androgen ablation therapy but also produce cross-resistance to other therapeutic modalities (3). Of particular importance are members of the BCL-2 family of cell death regulators, which are known to play evolutionarily conserved roles in the regulation of cell death in organisms ranging from the nematode *Caenorhabditis elegans* to humans (4). The family is subdivided into 3 major categories based on their functions in cell death regulation (4, 5). One subfamily (exemplified by BCL-2 itself and BCL-X_L) consists of cell death inhibitors and function to prevent the rate-limiting step in most examples of apoptosis (release of cytochrome c from mitochondria). The second (exemplified by Bax and Bak) are highly homologous to BCL-2 but function to directly promote cytochrome c release, possibly by forming transmembrane pores in the outer mitochondrial membrane. These proteins have been termed the "multidomain" proapoptotic BCL-2 family members, and expression of at least one of them appears to be required for initiation of apoptotic cell death. Finally, a third subfamily shares structural homology with the other two only within a circumscribed region (the so-called "BH3" domain), and these proteins appear to function either as inhibitors of the anti-apoptotic members of the family or as activators of Bax or Bak (6, 7). Overall, it appears that BH3 proteins function to promote the tetramerization of Bax and/or Bak, which generates a pore that is large enough to accommodate cytochrome c release (8). By virtue of their abilities to directly bind (and presumably neutralize) the BH3-only and multidomain family members, the effects of BCL-2 and BCL-X_L can be attributed to their functions as pore inhibitors.

Although the pore formation model is relatively simple and probably accounts for an important aspect of BCL-2 family protein functions, strong evidence is now available that indicates that pore formation is not enough to mediate cytochrome c release. Specifically, permeabilization of the outer mitochondrial membrane only releases approximately 15% of the total pool of cytochrome c, whereas up to 90% of the pool is released in cells dying by apoptosis (9, 10). Thus, cytochrome c release appears to commence via a two-step process. In the first step, a tightly bound pool of cytochrome c is mobilized, and in the second Bax/Bak pores allow for this mobilized cytochrome c to escape into the cytosol. It is possible that BH3-only proteins might use different domains to accomplish both effects, as has been shown in the case of a truncated form of the BH3-only protein, Bid (9). However, other work indicates that disruption of the electrostatic interactions between cytochrome c and the charged mitochondrial membrane lipid, cardiolipin, can also lead to cytochrome c mobilization (11).

BCL-2 is overexpressed in androgen-independent prostate cancers (12, 13), whereas expression of Bax may be reduced (13). Thus, understanding the molecular mechanisms underlying their effects on apoptosis should help to identify new therapeutic strategies to overcome the cell death resistance observed in androgen-independent disease. The overall goal of the research outlined in this project is to gain a better understanding of the effects of BCL-2 and Bax in prostate cancer cells. Our hypothesis is that an important component of the effects of these proteins is the regulation of intracellular calcium fluxes. More specifically, we suggest that proapoptotic members of the BCL-2 family promote release of calcium from its natural intracellular storage site (the endoplasmic reticulum), leading to increases in mitochondrial calcium that function to mobilize cytochrome c. Our model is summarized in **Figure 1.**

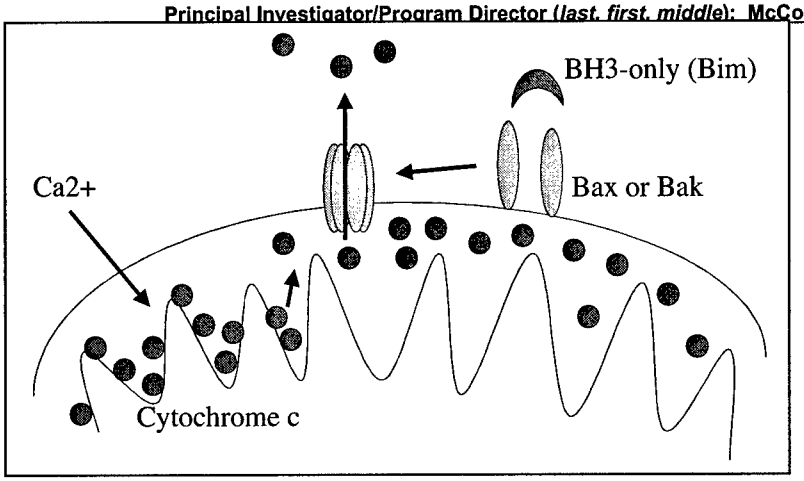

Figure 1: Two-step model for Ca2+-dependent cytochrome c release. Mitochondrial Ca2+ uptake "loosens" interactions between cytochrome c and the inner mitochondrial membrane, allowing for release via tetrameric Bax and/or Bak channels in the outer membrane. The effects of Ca2+ may be due to disruption of interactions between cytochrome c and cardiolipin or to more global changes in mitochondrial structure.

BODY

Observations leading to the present proposal:
In two previous studies we tested the hypothesis that Bax and Bak can target the ER to directly promote ER calcium release (14, 15). In the first study we overexpressed Bax or Bak in PC-3 cells via adenoviral transduction (14). (It should be noted that we did not directly manipulate BH3-only protein(s) in this study.) These cells displayed accumulation of Bax and Bak in both the ER and mitochondria, and kinetic analyses demonstrated that ER calcium levels were dramatically reduced roughly coincident with Bax or Bak protein expression. Depletion of the ER calcium pool was associated with increased calcium uptake by mitochondria, and selective or non-selective inhibitors of this uptake (BAPTA-AM or Ru-360) inhibited cytochrome c release and downstream events associated with cell death (caspase activation and DNA fragmentation).

These results were consistent with the hypothesis outlined in the model in Figure 1 above. However, we were concerned that the system was somewhat artificial, so we conducted a second study to examine whether or not Bax/Bak-dependent ER calcium release contributed to cytochrome c release and apoptosis induced by endogenous stimuli (15). We treated PC-3 cells with three different agents that are known to be potent inducers of apoptotic cell death (staurosporine, doxorubicin, and Fas) and measured the ER calcium pool size at various time points thereafter. Both staurosporine and doxorubicin caused a lowering of the ER calcium pool and increased mitochondrial calcium uptake prior to measurable cytochrome c release, caspase activation, and DNA fragmentation. Overexpression of BCL-2 blocked both ER calcium release and mitochondrial uptake, and the mitochondrial calcium uptake inhibitor (Ru-360) also inhibited cytochrome c release and cell death. Furthermore, studies in $Bax^{-/-}$ cells demonstrated that both ER calcium release and mitochondrial uptake were dependent on Bax.

Progress in the first year of funding:
Objective 1: *Define the effects of mitochondrial calcium uptake on cytochrome c mobilization and release.*
Tasks 1, 2: We have isolated mitochondria and membrane fractions from PC-3 cells using protocol-based and commercial isolation methods. Immunoblotting for organelle-specific target proteins confirmed that both methods work well, and low levels of exogenous calcium stimulate cytochrome c mobilization (measured by digitonin permeabilization) without causing the release of mitochondrial marker proteins. However, the yield obtained is poor and the approach will probably not be feasible for the planned $^{45}Ca2+$ uptake studies. We are therefore submitting an IACUC animal protocol describing the isolation of mitochondrial and microsomal (ER) fractions from mouse liver.

Task 3: We will wait to initiate the planned whole cell experiments until the organelle studies are complete.

Objective 2: *Determine the effects of BH3-only members of the BCL-2 family on intracellular calcium fluxes.* Task 1: We have defined the expression patterns of BH3-only proteins in LNCaP and PC-3 cells. In particular, both cell lines express Bim and Bid, the two proteins that we consider to be of highest importance for the proposed experiments.

Tasks 2-4: Two major issues arose over the past year that required us to address tasks outlined in Objectives 1-3 simultaneously (rather than in sequence as presented in the Statement of Work). First, work from Korsmeyer's laboratory and others argued that BCL-2 lowers the concentration of calcium in the ER lumen, thereby limiting the amount of calcium that could be released during apoptosis to be taken up by mitochondria (16). If reproduced, this observation would account for the effects of BCL-2 on ER calcium release and mitochondrial calcium uptake we observed in the previous two studies, but it would also undermine the idea that Bax and Bak target the ER to promote release during apoptosis. We therefore generated "stable" transfectants of PC-3 expressing wild-type, organelle-targeted (17), and mutant (BH4 deletion (18)) forms of BCL-2 to test their possible direct effects on the ER calcium pool and on cell death. The results demonstrated that basal levels of ER calcium (measured by releasing it with the ER calcium ATPase inhibitors, thapsigargin (19) and DBHQ (20)) were indistinguishable in cells transfected with vector or any of the BCL-2 constructs tested **(Figure 2).** Vector control cells or cells expressing cytosolic, mitochondrial, or BH4 mutant forms of BCL-2 challenged with either 1 μM staurosporine for 8 h or 1 μg/ml doxorubicin for 16 h displayed loss of ER calcium, whereas cells expressing either wild-type or ER-directed forms of BCL-2 did not **(Figure 2).** These agents also stimulated increases in mitochondrial calcium in the vector control cells or in cells transfected with cytosolic, mitochondrial, or BH4 mutant forms of BCL-2, whereas these increases were not observed in cells transfected with wild-type or ER-directed BCL-2 **(Figure 3).** Finally, staurosporine and doxorubicin induced significant increases in DNA fragmentation in vector controls as well as in cells expressing cytosolic, mitochondrial, or BH4 mutant forms of BCL-2, responses that were strongly inhibited by either wild-type or ER-directed forms of BCL-2 **(Figure 4).** Together, these results demonstrate that BCL-2 functions at the ER (not the mitochondria) to directly inhibit the ER calcium release and subsequent mitochondrial calcium uptake caused by some pro-apoptotic stimuli. These experiments.

We then began studies aimed at determining the effects of proapoptotic stimuli on the localization of the BH3-only protein, Bim, and the multi-domain Bax protein. Our reasons for focusing on Bim and Bax were based on the observation that Bim (like Bid) is capable of directly activating Bax (6, 7), and Bax-null cells displayed defects in ER calcium mobilization in our previous studies (15). In preliminary experiments we confirmed that PC-3 cells express Bim. We also obtained GFP-conjugated forms of wild-type and mutant Bax (C-terminal domain mutants) from Dr. Richard Youle (NIH) and confirmed that we could accurately measure their subcellular localization in single cells by confocal microscopy. It was in the course of conducting these experiments that we encountered an unexpected problem. As a control, we stained our transfectants with an anti-BCL-2 antibody to confirm that the targeted mutants localized correctly in intact cells. (We had already confirmed that they localized correctly using organelle fractionation.) BCL-2 levels were quantified at the single cell level by flow cytometry or by laser scanning cytometry (LSC). Surprisingly, PC-3 cells transfected with mitochondrial BCL-2 lost the protein with rapid kinetics, and essentially all of the transfected protein was gone by 21 days after expansion of stable clones **(Figure 5).** Wild-type and ER-targeted forms of BCL-2 were retained longer but were still lost with a t1/2 of approximately 14 days (Figure 5). Expression of the cytosolic form of BCL-2 was more stable **(Figure 5),** but the protein moved from the cytosol to the nucleus after about 21 days (data not shown). Transient transfection of either the mitochondrial or BH4 mutant forms directly stimulated cell death, but the wild-type and ER-targeted forms did not (data not shown). These findings make us concerned that overexpression studies like the ones proposed in our Statement of Work, Objective 2, Tasks 3 and 4, may not provide as much insight into the functions of the various BCL-2 family proteins as targeted knockdown experiments would. The loss of wild-type BCL-2 displayed by the PC-3 cells is also worrisome given that the protein is thought to play a positive role in prostate cancer progression and androgen-independent

growth. Similar effects have not been reported in LNCaP cells transfected with BCL-2, and orthotopically selected metastatic variants of LNCaP display stable overexpression of the protein relative to parental LNCaP cells or non-metastatic variants.

To overcome these problems we have implemented two complementary strategies. First, we have generated stable transfectants of LNCaP-Pro5 cells expressing wild-type or mutant forms of BCL-2 under the control of an autologous (CMV-driven) promoter and an inducible (ecdysone-driven) promoter. LNCaP-Pro5 cells are more difficult to load with our calcium-sensitive fluorescent indicators, but LNCaP cells are generally considered a more appropriate model of human prostate cancer than are PC-3 cells. Second, we are optimizing our techniques for knocking down expression of target genes by siRNA in these cells. We have successfully knocked down two control proteins ($p21^{WAF-1/Cip-1}$ and $p27^{Kip-1}$), and these data were used in two manuscripts that have been submitted for publication (see Appendix). **It is our plan to make the gene silencing experiments described under Objective 2, Task 5 the top priority in the coming 6 months.** Specifically, we will directly test whether or not Bim-mediated Bax activation controls ER calcium release in LNCaP-Pro5 cells and determine how BCL-2 affects these processes.

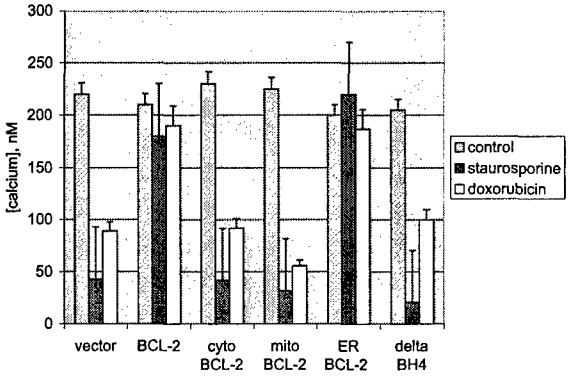

Figure 2: Effects of various forms of BCL-2 on ER calcium stores. Endoplasmic reticular calcium was measured indirectly in fura-2-labelled cells by thapsigargin or DBHQ-mediated release. Mean ± S.D., n = 3.

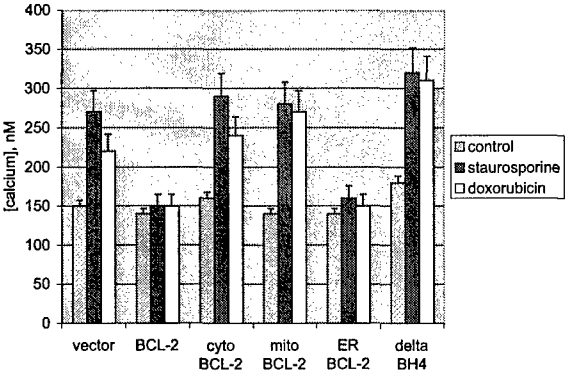

Figure 3: Effects of various forms of BCL-2 on mitochondrial calcium uptake. Mitochondrial calcium levels were measured using the fluorescent probe, Rhod-2 AM. Mean ± S.D., n = 3.

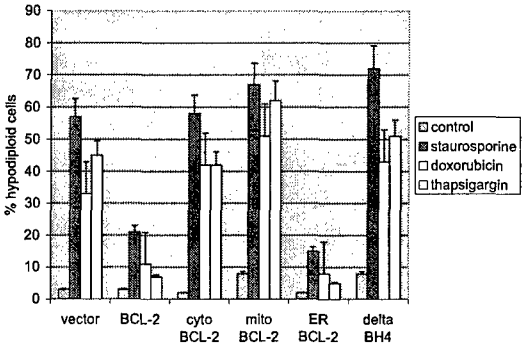

Figure 4: Effects of various forms of BCL-2 on cell death. Apoptosis was measured at 24 h by propidium iodide staining and FACS analysis. Mean ± S.D., n = 3.

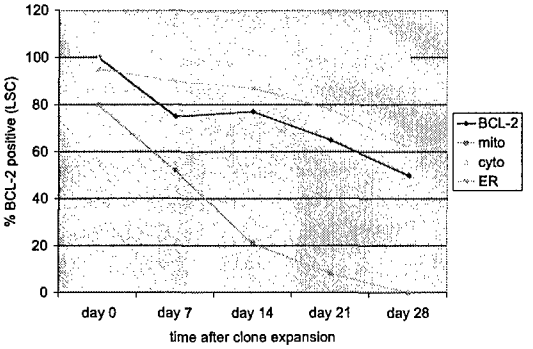

Figure 5: Loss of BCL-2 with time in culture. Cells were maintained in 1 mg/ml G418 throughout the course of the experiment. Results are representative of 3 independent transfection experiments. Similar effects were observed in clones isolated by limiting dilution subcloning.

Objective 3: *Identify the effects of Bax and Bak on ER calcium fluxes.*

Task 1: We are optimizing our organelle preparations as described under Objective 1 above. We have also discussed collaborating with Dr. Richard Youle at NIH to obtain recombinant Bax and Bak. (He has generated both proteins and is willing to work with us on this project.)

Tasks 2 and 3: As discussed above, we are concerned that the strategies we have used to overexpress targeted forms of BCL-2 to the ER or mitochondria have perturbed cell function(s) in inappropriate ways. Thus, we do not plan to begin generating targeted forms of Bax and Bak until we have confirmed that one or both proteins normally localize to the ER in whole cells.

KEY RESEARCH ACCOMPLISHMENTS

- Obtained very strong evidence for the idea that BCL-2 must be localized to the ER to prevent apoptosis-associated calcium fluxes in PC-3 cells.
- Demonstrated that BCL-2 does not reduce ER luminal calcium levels in these cells
- Showed that, contrary to our expectations, mitochondrial BCL-2 does not protect cells from death
- Showed that exogenous calcium can promote mobilization of cytochrome c from tightly bound mitochondrial pools, consistent with the model presented in Figure 1
- Have established the appropriate conditions for successful gene silencing in LNCaP-Pro5 cells and used these methods to complete two other prostate cancer research papers (Appendix)

REPORTABLE OUTCOMES

1. Generated transfectants of PC-3 and LNCaP-Pro5 expressing various forms of BCL-2.
2. Used siRNA methods developed within the context of this grant to address reviewers' comments on a manuscript, "Bortezomib abolishes TRAIL resistance via a p21-dependent mechanism in human bladder and prostate cancer cells," L. Lashinger, K. Zhu, et al., *Cancer Research* (Advances in Brief). (Keyi Zhu's graduate stipend is directly supported by this grant.)
3. Used siRNA methods to complete a second manuscript, "The proteasome inhibitor bortezomib interferes with docetaxel-induced apoptosis in human LNCaP-Pro5 prostate cancer cells," S. Canfield et al, *Clinical Cancer Research.* (Revisions pending.)

CONCLUSIONS

1. The suppression of ER calcium release observed in prostate cancer cells that overexpress BCL-2 is not caused by a lowering of luminal calcium levels.
2. The pool of BCL-2 that is localized to the ER plays an important role in controlling ER calcium efflux during apoptosis.
3. Overexpression of BCL-2 targeted to mitochondria is not tolerated.
4. Overexpression of a BH4 mutant form of BCL-2 appears to promote ER calcium efflux.
5. Calcium can promote cytochrome c mobilization in isolated mitochondria.

REFERENCES

1. Jemal, A., Tiwari, R. C., Murray, T., Ghafoor, A., Samuels, A., Ward, E., Feuer, E. J., and Thun, M. J. Cancer statistics, 2004. CA Cancer J Clin, *54:* 8-29, 2004.
2. Assikis, V. J. and Simons, J. W. Novel therapeutic strategies for androgen-independent prostate cancer: an update. Semin Oncol, *31:* 26-32, 2004.
3. Bruckheimer, E. M., Gjertsen, B. T., and McDonnell, T. J. Implications of cell death regulation in the pathogenesis and treatment of prostate cancer. Semin Oncol, *26:* 382-398, 1999.
4. Danial, N. N. and Korsmeyer, S. J. Cell death: critical control points. Cell, *116:* 205-219, 2004.
5. Chao, D. T. and Korsmeyer, S. J. BCL-2 family: regulators of cell death. Annu Rev Immunol, *16:* 395-419, 1998.

6. Letai, A., Bassik, M. C., Walensky, L. D., Sorcinelli, M. D., Weiler, S., and Korsmeyer, S. J. Distinct BH3 domains either sensitize or activate mitochondrial apoptosis, serving as prototype cancer therapeutics. Cancer Cell, *2:* 183-192, 2002.
7. Kuwana, T., Bouchier-Hayes, L., Chipuk, J. E., Bonzon, C., Sullivan, B. A., Green, D. R., and Newmeyer, D. D. BH3 Domains of BH3-Only Proteins Differentially Regulate Bax-Mediated Mitochondrial Membrane Permeabilization Both Directly and Indirectly. Mol Cell, *17:* 525-535, 2005.
8. Wei, M. C., Lindsten, T., Mootha, V. K., Weiler, S., Gross, A., Ashiya, M., Thompson, C. B., and Korsmeyer, S. J. tBID, a membrane-targeted death ligand, oligomerizes BAK to release cytochrome c. Genes Dev, *14:* 2060-2071, 2000.
9. Scorrano, L., Ashiya, M., Buttle, K., Weiler, S., Oakes, S. A., Mannella, C. A., and Korsmeyer, S. J. A distinct pathway remodels mitochondrial cristae and mobilizes cytochrome c during apoptosis. Dev Cell, *2:* 55-67, 2002.
10. Scorrano, L. and Korsmeyer, S. J. Mechanisms of cytochrome c release by proapoptotic BCL-2 family members. Biochem Biophys Res Commun, *304:* 437-444, 2003.
11. Ott, M., Robertson, J. D., Gogvadze, V., Zhivotovsky, B., and Orrenius, S. Cytochrome c release from mitochondria proceeds by a two-step process. Proc Natl Acad Sci U S A, *99:* 1259-1263, 2002.
12. McDonnell, T. J., Troncoso, P., Brisbay, S. M., Logothetis, C., Chung, L. W., Hsieh, J. T., Tu, S. M., and Campbell, M. L. Expression of the protooncogene bcl-2 in the prostate and its association with emergence of androgen-independent prostate cancer. Cancer Res, *52:* 6940-6944, 1992.
13. McConkey, D. J., Greene, G., and Pettaway, C. A. Apoptosis resistance increases with metastatic potential in cells of the human LNCaP prostate carcinoma line. Cancer Res, *56:* 5594-5599, 1996.
14. Nutt, L. K., Pataer, A., Pahler, J., Fang, B., Roth, J., McConkey, D. J., and Swisher, S. G. Bax and Bak promote apoptosis by modulating endoplasmic reticular and mitochondrial Ca2+ stores. J Biol Chem, *277:* 9219-9225, 2002.
15. Nutt, L. K., Chandra, J., Pataer, A., Fang, B., Roth, J. A., Swisher, S. G., O'Neil, R. G., and McConkey, D. J. Bax-mediated Ca2+ mobilization promotes cytochrome c release during apoptosis. J Biol Chem, *277:* 20301-20308, 2002.
16. Oakes, S. A., Opferman, J. T., Pozzan, T., Korsmeyer, S. J., and Scorrano, L. Regulation of endoplasmic reticulum Ca2+ dynamics by proapoptotic BCL-2 family members. Biochem Pharmacol, *66:* 1335-1340, 2003.
17. Zhu, W., Cowie, A., Wasfy, G. W., Penn, L. Z., Leber, B., and Andrews, D. W. Bcl-2 mutants with restricted subcellular location reveal spatially distinct pathways for apoptosis in different cell types. Embo J, *15:* 4130-4141, 1996.
18. Reed, J. C., Zha, H., Aime-Sempe, C., Takayama, S., and Wang, H. G. Structure-function analysis of Bcl-2 family proteins. Regulators of programmed cell death. Adv Exp Med Biol, *406:* 99-112, 1996.
19. Lam, M., Dubyak, G., Chen, L., Nunez, G., Miesfeld, R. L., and Distelhorst, C. W. Evidence that BCL-2 represses apoptosis by regulating endoplasmic reticulum-associated Ca2+ fluxes. Proc Natl Acad Sci U S A, *91:* 6569-6573, 1994.
20. Moore, G. A., McConkey, D. J., Kass, G. E., O'Brien, P. J., and Orrenius, S. 2,5-Di(tert-butyl)-1,4-benzohydroquinone--a novel inhibitor of liver microsomal Ca2+ sequestration. FEBS Lett, *224:* 331-336, 1987.

The proteasome inhibitor bortezomib interferes with docetaxel-induced apoptosis in human prostate cancer cells.

Steven E. Canfield[1,2], Keyi Zhu[2], Simon A. Williams[2], and David J. McConkey[2]

Departments of [1]Urology and [2]Cancer Biology,

UT MD Anderson Cancer Center, Houston, Texas 77030

Running title: Bortezomib interferes with docetaxel

Key words: Velcade, PS-341, p21, Taxotere, LNCaP

Address correspondence to:
David McConkey
Department of Cancer Biology – 173
UT MD Anderson Cancer Center
1515 Holcombe Boulevard
Houston, Texas 77030
Tel. (713) 792-8591
FAX (713) 792-8747
Email: dmcconke@mdanderson.org

Abstract

Bortezomib (PS-341, Velcade) is a peptide boronate inhibitor of the 20S proteasome that is currently being combined with taxanes in several clinical trials. Here we demonstrate that exposure of human LNCaP-Pro5 prostate cancer cells to bortezomib plus docetaxel (Taxotere) resulted in less apoptosis than was observed in cells exposed to docetaxel alone. The effects of bortezomib were associated with accumulation of p21 and abrogation of docetaxel-induced M-phase arrest and were mimicked by chemical cyclin-dependent kinase (cdk) inhibitors. Transient transfection of LNCaP-Pro5 cells with p21 also inhibited docetaxel-induced apoptosis, and elimination of p21 expression via siRNA eliminated the bortezomib-induced inhibition of docetaxel-induced apoptosis. Together, our results demonstrate that bortezomib interferes with docetaxel-induced apoptosis via a p21-dependent mechanism. These observations may have important implications for the ongoing bortezomib-docetaxel combination trials as well as trials employing bortezomib and other cell cycle-sensitive agents.

(139 words)

Introduction

In 2004, prostate cancer is the most common cancer in men, with an estimated incidence of over 230,000 new cases, and the second most lethal cancer in men, with almost 30,000 new deaths.(1) Advanced disease has a 5-year survival of only 30%.(2) Historically, chemotherapy has been utilized with palliative intent but unclear survival benefit for these advanced stage patients. Current practices for hormone-refractory, metastatic prostate cancer incorporate the use of taxanes. Docetaxel in particular is being incorporated in numerous current clinical trials either as a single or combination agent against androgen independent prostate cancer, and it is also being investigated for its use as a neoadjuvant or adjuvant agent in hormone sensitive, locally aggressive prostate cancer.(5, 6) Combination regimens involving docetaxel and well-established agents such as estramustine and prednisone are being evaluated, but it appears that these strategies are not yielding a qualitative increase in anti-tumor activity. Thus, the development of novel combination approaches involving docetaxel and biological targeting agents is being pursued aggressively.

The activity of the 26S proteasome is required for cell cycle progression and cell survival, making it an attractive therapeutic target in cancer. Bortezomib (also know as PS-341 or Velcade) is a dipeptidyl boronic acid inhibitor of the chymotryptic activity of the proteasome that is currently the only proteasome inhibitor in clinical use. In preclinical studies the drug displayed promising activity in the National Cancer Institute's (NCI) 60 cancer cell line panel, with a mean IC_{50} of 7nM and a unique cytotoxic profile compared to historical results of 60,000 other compounds.(10) The drug has especially impressive activity in multiple myeloma and recently received FDA approval for the

treatment of this disease,(11, 12) Bortezomib also exhibited activity in preclinical models of human solid tumors, especially when combined with standard chemotherapeutic agents, including docetaxel .(14, 15) Bortezomib has been utilized in 60 clinical trials, most currently ongoing. It is being combined with docetaxel in 5 of these trials, including one for prostate cancer. Knowledge about the interactions of these two agents has current relevance for clinical application.

Here we characterized the effects of bortezomib on docetaxel-induced apoptosis in androgen-sensitive LNCaP-Pro5 cells. The results demonstrate that bortezomib prevents docetaxel-induced accumulation of cells in M phase and subsequent apoptosis via a p21-dependent mechanism. Our findings represent a cautionary note for the development of other combinations of bortezomib with cell cycle-sensitive therapeutic approaches.

Materials and Methods

Animals, Cell Lines and Antibodies

Male nude mice (BALB/c) were purchased from the Animal Production Area of the National Cancer Institute Frederick Cancer Research and Development Center (Frederick, MD). LNCaP Pro5 human prostate cancer cells were derived from orthotopic recycling of the parental line.(16) Briefly, the parental cell line (LNCaP, American Type Culture Collection, Rockville, MD) was orthotopically injected into the prostates of nude mice, and the resultant prostate tumors were harvested, mechanically dissociated and regrown in culture. These cells were then reimplanted into the prostates of nude mice,

and the recycling process was continued for a total of 5-cycles to produce the more locally aggressive variant LNCaP-Pro5. Cells were maintained in RPMI supplemented with 10% fetal bovine serum (FBS) along with sodium pyruvate, nonessential amino acids, L-glutamine, vitamins and antibiotics under conditions of 5% CO_2 in air at 37°C. Antibodies were obtained from the following commercial sources: anti-p21 and p27 (Transduction Laboratories, San Diego, CA), anti-actin (Sigma Chemical Co., St. Louis, MO)

MTT Assays

Cells were cultured in 96-well plates (10,000 cells/well) and rested for 48 hours. Following incubation with escalating doses of bortezomib alone (1.25 – 20nM) or combined with docetaxel 10ng/mL, or escalating doses of docetaxel alone (1.25 – 20ng/mL) or combined with bortezomib 10nM, for 48 hours, cells were incubated with MTT (3-[4,5-dimethylthiazol-2-y])-2,5-diphenyltetrazolium bromide (Sigma Chemical Co., St. Louis, MO) in PBS at 5mg/mL, (10uL/well) for 2 hours at 37°C. The medium was replaced with DMSO (40uL/well) and MTT precipitates were dissolved for 1 hour before quantification of optical densities (570nm).

Quantification of DNA Fragmentation

DNA fragmentation was measured by propidium iodide (PI) staining and fluorescence-acivated cell sorting (FACS) analysis. Cells were plated in six-well plates (1×10^4 cells/well). Following incubation with 1 – 100 nM bortezomib, 1 – 100 ng/mL docetaxel,

25uM roscovitine, 100uM olomucine or combinations, either alone or in combination with p21 or p27 amplification or silencing transfections *in vitro*, cells were harvested, pelleted by centrifugation, and resuspended in PBS containing 50ug/mL PI, 0.1% Triton X-100, and 0.1% sodium citrate. Cells were incubated with the PI solution for at least 1 hour at 4°C, and flow cytometric analysis was performed with a FACScan (Beckman-Coulter, ...).

Immunoblotting

Cells (1 x 10^5) were incubated with 100nM bortezomib, 100ng/mL docetaxel or the combination, either alone or after exposure to transfections with control vector, p21 cDNA, nonspecific siRNA, p21 siRNA or p27 siRNA. Cells were lysed with 1% Triton X-100 buffer *in situ* for 10 minutes, then transferred after scraping to eppindorf tubes where lysis continued for 1 hour at 4°C. Lysates were centrifuged at high speed to exclude the cellular pellet, and protein concentration was determined with Bradford odensitometry. Approximately 20ug from each sample were subjected to SDS-PAGE, proteins were transferred to nitrocellulose membranes, and the membranes were blocked with 5% nonfat milk in a Tris-buffered saline solution containing 0.1% Tween 20 for 2 hours at 4°C. Blots were then probed overnight with the relevant antibodies, washed, and probed with species-specific secondary antibodies coupled to horseradish peroxidase. Immunoreactive material was was detected by chemiluminescence (Amersham...).

Immunofluorescence and DNA Fragmentation

p21 expressing cells were identified by FITC labeling and FACS analysis, which was combined with PI staining for quantification of DNA fragmentation. Cells were plated in six-well plates (1 x 10^4 cells/well). Following incubation with 100 nM bortezomib, 100 ng/mL docetaxel, or combinations, either alone or in combination with p21 or p27 amplification or silencing transfections *in vitro*, cells were harvested, pelleted by centrifugation, washed in phosphate buffered saline (PBS), and resuspended in 1% paraformaldehyde for 10 minutes at room temperature. Cells were then washed in PBS, centrifuged, and resuspended in intracellular staining buffer (ISB) with 0.1% Tritin X-100 and relevant primary antibody (e.g., monoclonal anti-p21 antibody at 1:100 dilution) for 1 hour at 4°C. Cells were then washed in ISB, centrifuged, and resuspended in ISB with species-specific secondary FITC (e.g., rabbit anti-mouse at 1:50 dilution) for 30 minutes at 4°C under light protection. Cells were then washed with ISB, centrifuged, and resuspended in PI solution as mentioned above, overnight at 4°C under light protection. Cytometric analysis was performed as mentioned above, quantifying DNA fragmentation for populations of all, p21 expressing and p21 nonexpressing cells as separated by FITC label.

Results

Effects of bortezomib and docetaxel on cell proliferation and apoptosis . We compared the concentration-dependent effects of bortezomib, docetaxel, or both agents on the proliferation of LNCaP-Pro5 cells using MTT assays. Consistent with previous work (10),(17), bortezomib inhibited cell proliferation at low nanomolar concentrations

(IC_{90} = 10nM) (Fig. 1A). Docetaxel also inhibited cell proliferation in a concentration-dependent fashion (IC_{90} = 10ng/mL) (Fig. 1B). When cells were treated first with a fixed concentration of docetaxel (10ng/mL) followed by increasing concentrations of bortezomib (1.25 – 20 nM), no significant change in growth suppression was seen compared to that observed with docetaxel alone. (Fig. 1A) Likewise, when cells were treated first with a fixed concentration of bortezomib (10nM) followed by increasing concentrations of docetaxel, the level of growth suppression was similar to that observed in response to treatment with bortezomib alone. (Fig 1B)

We next measured the effects of the bortezomib plus docetaxel on DNA fragmentation typical of apoptosis by propidium iodide staining and FACS analysis. Cells treated with either bortezomib (10 nM) or docetaxel (10 ng/mL) displayed significant DNA fragmentation 48 h after drug exposure (45 and 68%, respectively)(Fig. 1C,D) However, when cells were first treated with docetaxel (10ng/mL) followed by increasing concentrations of bortezomib (1 – 10nM), a significant reduction in docetaxel-induced apoptosis occurred as the concentration of bortezomib dose increased (50% reduction) (Fig. 1C). Likewise, when cells were first treated with bortezomib (10nM) followed by increasing concentrations of docetaxel (1 – 10ng/mL), the levels of DNA fragmentation observed were identical to levels achieved in cells treated with bortezomib alone, representing a 50% reduction in the docetaxel response (Fig. 1D)

Chemical cdk inhibitors mimic the effects of bortezomib. Docetaxel-induced apoptosis occurs during the M phase of the cell cycle.(18) The PI/FACS results obtained above demonstrated that bortezomib completely blocked docetaxel-induced accumulation of cells in M phase (data not shown). In a previous study we showed that bortezomib

inhibits basal and docetaxel-induced cdk2 and cdc2 activation (Nawrocki), so we examined whether or not chemical cdk inhibitors might also prevent M phase accumulation and apoptosis. Consistent with our prediction, roscovitine (25 μM)(Fig. 2A) and olomoucine (100μM) (Fig. 2B) both inhibited docetaxel –induced M-phase accumulation (data not shown) and apoptosis. These data indicate that bortezomib's ability to block cdk activation is sufficient to explain its antagonism of docetaxel-induced M phase arrest and apoptosis in LNCaP-Pro5 cells.

Role of p21. In a previous study we showed that bortezomib promotes the accumulation of p53 and p21 in LNCaP-Pro5 cells (refs). It therefore seemed reasonable that p21 might contribute to the bortezomib-induced inhibition of M phase accumulation in docetaxel-treated cells. In a first series of experiments we exposed LNCaP-Pro5 cells to bortezomib, docetaxel, or a combination of both agents for 24 h and measured p21 expression by immunoblotting. Consistent with our expectations, p21 levels were markedly elevated in cells exposed to bortezomib or bortezomib plus docetaxel (Fig. 2A). At the 24 h time point the bortezomib-mediated antagonism of docetaxel-induced apoptosis was even more obvious than it was at 48 h (Fig. 2B), presumably because docetaxel-induced apoptosis occurred with more rapid kinetics than bortezomib-induced apoptosis.

To more directly implicate p21 in the process, we transiently transfected LNCaP-Pro5 cells with a p21 expression vector to mimic the expression seen after exposure to bortezomib. Parallel control experiments demonstrated that transfection efficiency was approximately 20% (data not shown). Cells tranfected with p21 displayed significantly lower levels of apoptosis than were observed in cells transfected with empty vector (Fig.

4A) Parallel immunoblotting studies confirmed that the transfected cells expressed higher levels of p21 protein (Fig. 4B).

In order to further explore the role of p21 in the effects of bortezomib, we used two-color FACS to compare the levels of apoptosis observed in p21-positive and p21-negative subsets of LNCaP-Pro5 cells (Fig. 6A). Consistent with the immunoblotting results, untreated cells or cells treated with docetaxel alone (100ng/mL) for 24 hours did not express significant levels of p21, while 70% of cells treated with bortezomib (100nM) or bortezomib + docetaxel for 24 hours expressed elevated p21 levels (Fig. 5). By gating on these subsets we determined the percentages of apoptotic p21-positive and p21-negative cells by PI/FACS. The control cells and those exposed to docetaxel displayed identical levels of DNA fragmentation in the ungated population and the p21-negative subset because the percentage of p21-positive cells within the bulk population was so low (Fig. 6B). However, in cells treated with either bortezomib alone or bortezomib plus docetaxel, very little apoptosis was detected in the p21-positive subset, whereas levels of apoptosis were high in the 30% of cells that did not express p21 (Fig. 6B). Therefore, expression of p21 correlated directly with resistance to apoptosis in cells treated with either bortezomib alone or bortezomib plus docetaxel.

Requirement for p21 in bortezomib-mediated inhibition of docetaxel-induced apoptosis. The results presented above strongly suggested that p21-mediated inhibition of cdk activation accounted for the inhibition of M phase arrest and apoptosis observed in LNCaP-Pro5 cells treated with docetaxel plus bortezomib. To directly test this possibility, we examined the effects of silencing p21 expression on apoptosis in cells treated with bortezomib plus docetaxel. In control cells, significant inhibition of

docetaxel-induced apoptosis was seen when bortezomib (100nM) was combined with docetaxel (100ng/mL) after 24 hours. (Fig. 7A) However, in p21 silenced cells, the bortezomib-mediated antagonism was reversed and the levels of apoptosis were equivalent to those observed in cells treated with docetaxel alone. (Fig. 7A) Immunoblotting confirmed that the siRNA construct eliminated p21 expression under all conditions (Fig. 7B). These results directly confirm that bortezomib-induced accumulation of p21 mediates its antagonistic effects on docetaxel-induced apoptosis.

Discussion

Given the challenge of advanced prostate cancer therapy, novel agents with promising activity are quickly incorporated into trials which often include conventional agents as well. Bortezomib, a potent inhibitor of the 26S proteasome, has shown significant activity against both androgen-sensitive and androgen-independent prostate cancer in preclinical models.(10, 22) A recently completed Phase I clinical trial of bortezomib in patients with advanced prostate cancer demonstrated its potential for this disease.(23) Paclitaxel has a well established role in advanced prostate cancer,(24-26) and docetaxel is currently under investigation as an equivalent or superior substitute.(24, 27-29) Results of Phase II clinical trials of docetaxel based combination regimens have shown clear palliative responses, decreases in PSA levels by at least 50% in at least 60% of patients, and suggestions of improved survival.(27) Docetaxel also holds promise in the early stages of prostate cancer progression, and is currently under investigation for its role as a neoadjuvant or adjuvant agent in aggressive, androgen-sensitive prostate

cancer.(5, 6, 30-32) Furthermore, docetaxel based regimens are actively being developed to incorporate novel investigational agents, such as a current clinical trial with bortezomib in advanced prostate cancer. Docetaxel effects many cellular pathways and is therefore thought to have excellent potential for synergy with novel anti-cancer agents.(33) Promising targets have included the EGF receptor(34), HER-2 (35-38), the farnesyl transferase pathway(39), and Bcl-2.(40, 41) The proteasome is a target under current investigation in 5 clinical trials with combination docetaxel, but is as yet of unproven benefit.

The results of this study demonstrate that bortezomib's activity as a strong cell cycle inhibitor produce antagonistic effects on apoptosis when it is combined with taxanes. The effects of bortezomib were mediated by its ability to promote accumulation of the cdk inhibitor, p21, and studies with chemical cdk inhibitors (roscovitine, olomoucine) strongly suggest that the mechanism also involved p21-mediated cdk inhibition. Previous studies have demonstrated that taxanes initiate apoptosis in cells that are initially arrested at M phase (refs) and that taxane-induced apoptosis requires cdc2 activation (refs). Our observations are entirely consistent with these results. Although the drug has clear antagonistic effects on docetaxel-induced apoptosis in this model and others (Nawrocki), some studies have reported that bortezomib sensitizes other cells to taxane-induced apoptosis (Chiao), so it is possible that a characterization of the molecular mechanisms involved in the different responses will allow for the identification of patients who would benefit from combination therapy. Furthermore, bortezomib's ability to arrest cells at G_1/S and G_2 may be an effect that can be exploited with other pro-apoptotic stimuli, particularly TRAIL (refs).

Although bortezomib clearly inhibited docetaxel-induced apoptosis in the LNCaP-Pro5 cells, the levels of apoptosis observed in cells treated with bortezomib alone were identical to those observed in cells treated with bortezomib plus increasing concentrations of docetaxel, demonstrating that docetaxel did not interfere with bortezomib-induced apoptosis. Given that bortezomib arrests cells at earlier point(s) in the cell cycle, this result is not surprising, and it strongly suggests that antagonism will only be observed in tumor cells that are more sensitive to apoptosis induced by taxanes versus bortezomib. Although the molecular mechanisms underlying bortezomib-induced apoptosis remain unclear, candidates include inhibition of NFkB (refs), p53 activation (Williams), production of reactive oxygen species (refs), and the accumulation of misfolded and/or damaged proteins resulting in a phenomenon termed "ER stress" (refs). It is interesting to note that levels of bortezomib-induced apoptosis were significantly higher in the 30% of cells that were p21-negative in bulk populations (Fig. 6) and that they were also higher following p21 silencing (Fig. 7). Thus, it does not appear that p21 is required for bortezomib-induced apoptosis, and in fact strategies to inhibit p21 expression in tumors will probably enhance the drug's activity.

It is also important to point out that tumor cell apoptosis is only one of the mechanisms underlying tumor growth inhibition in vivo. For example, in our own previous work we demonstrated that treatment of human L3.6pl pancreatic cancer cells with bortezomib plus docetaxel resulted lower levels of clonogenic survival (measured at 14 days) as compared to those observed in cells treated with either bortezomib or docetaxel alone. Treatment with the combination also resulted in stronger inhibition of tumor growth than did therapy with either single agent in orthotopic L3.6pl tumor

xenografts, effects that were linked to strong inhibition of tumor cell proliferation and angiogenesis (Nawrocki). Thus, the fact that bortezomib and taxanes inhibit cell cycle progression at different points and inhibit angiogenesis via different molecular mechanisms probably explains why combination therapy is more potent when the assays of drug activity are highly sensitive to changes in tumor cell proliferation. However, if the goal of therapy is to regress established bulky disease, then caution should be exercised before proceeding with this or other combinations of bortezomib and cell cycle-sensitive agents. While inhibition of proliferation and/or angiogenesis is expected to produce disease stabilization, it does not appear that these effects are generally sufficient to produce regressions. Conversely, levels of therapy-induced apoptosis do appear to predict response in tumors treated with cytotoxic agents (Davis). It is possible that bortezomib's antagonism of docetaxel-induced apoptosis can be overcome, for example by silencing p21 expression. Alternatively, it may be better to optimize scheduling or identify combination regimens that better exploit bortezomib's complex effects on the cell cycle.

REFERENCES

1. Jemal, A., Tiwari, R. C., Murray, T., Ghafoor, A., Samuels, A., Ward, E., Feuer, E. J., and Thun, M. J. Cancer statistics, 2004. CA Cancer J Clin, *54:* 8-29, 2004.
2. Kessler, B. and Albertsen, P. The natural history of prostate cancer. Urol Clin North Am, *30:* 219-226, 2003.
3. Canil, C. M. and Tannock, I. F. Is there a role for chemotherapy in prostate cancer? Br J Cancer, 2004.
4. Nehme, A., Varadarajan, P., Sellakumar, G., Gerhold, M., Niedner, H., Zhang, Q., Lin, X., and Christen, R. D. Modulation of docetaxel-induced apoptosis and cell cycle arrest by all- trans retinoic acid in prostate cancer cells. Br J Cancer, *84:* 1571-1576, 2001.
5. Dreicer, R. and Klein, E. A. Preliminary observations of single-agent docetaxel as neoadjuvant therapy for locally advanced prostate cancer. Semin Oncol, *28:* 45-48, 2001.
6. Oh, W. K., George, D. J., Kaufman, D. S., Moss, K., Smith, M. R., Richie, J. P., and Kantoff, P. W. Neoadjuvant docetaxel followed by radical prostatectomy in patients with high-risk localized prostate cancer: a preliminary report. Semin Oncol, *28:* 40-44, 2001.
7. Adams, J. The proteasome: structure, function, and role in the cell. Cancer Treat Rev, *29 Suppl 1:* 3-9, 2003.
8. Kisselev, A. F. and Goldberg, A. L. Proteasome inhibitors: from research tools to drug candidates. Chem Biol, *8:* 739-758, 2001.

9. LeBlanc, R., Catley, L. P., Hideshima, T., Lentzsch, S., Mitsiades, C. S., Mitsiades, N., Neuberg, D., Goloubeva, O., Pien, C. S., Adams, J., Gupta, D., Richardson, P. G., Munshi, N. C., and Anderson, K. C. Proteasome inhibitor PS-341 inhibits human myeloma cell growth in vivo and prolongs survival in a murine model. Cancer Res, *62:* 4996-5000, 2002.

10. Adams, J., Palombella, V. J., Sausville, E. A., Johnson, J., Destree, A., Lazarus, D. D., Maas, J., Pien, C. S., Prakash, S., and Elliott, P. J. Proteasome inhibitors: a novel class of potent and effective antitumor agents. Cancer Res, *59:* 2615-2622, 1999.

11. Richardson, P. G., Barlogie, B., Berenson, J., Singhal, S., Jagannath, S., Irwin, D., Rajkumar, S. V., Srkalovic, G., Alsina, M., Alexanian, R., Siegel, D., Orlowski, R. Z., Kuter, D., Limentani, S. A., Lee, S., Hideshima, T., Esseltine, D. L., Kauffman, M., Adams, J., Schenkein, D. P., and Anderson, K. C. A phase 2 study of bortezomib in relapsed, refractory myeloma. N Engl J Med, *348:* 2609-2617, 2003.

12. Kane, R. C., Bross, P. F., Farrell, A. T., and Pazdur, R. Velcade: U.S. FDA approval for the treatment of multiple myeloma progressing on prior therapy. Oncologist, *8:* 508-513, 2003.

13. Lenz, H. J. Clinical update: proteasome inhibitors in solid tumors. Cancer Treat Rev, *29 Suppl 1:* 41-48, 2003.

14. Pink M, P. C., Worland P, et. al. PS-341 enhances chemotherapeutic effects in human xenograph models. Proceedings of the American Association of Cancer Research, *43:* 158, 2002.

15. Gumerlock PH, M. L., Lau AH, et al. Docetaxel followed by PS-341 results in phosphorylation and stabilization of p27 and increases response in non-small cell lung carcinoma (NSCLC). Clinical Cancer Research, *7:* 157, 2001.

16. Pettaway, C. A., Pathak, S., Greene, G., Ramirez, E., Wilson, M. R., Killion, J. J., and Fidler, I. J. Selection of highly metastatic variants of different human prostatic carcinomas using orthotopic implantation in nude mice. Clin Cancer Res, *2:* 1627-1636, 1996.

17. Williams, S., Pettaway, C., Song, R., Papandreou, C., Logothetis, C., and McConkey, D. J. Differential effects of the proteasome inhibitor bortezomib on apoptosis and angiogenesis in human prostate tumor xenografts. Mol Cancer Ther, *2:* 835-843, 2003.

18. Ringel, I. and Horwitz, S. B. Studies with RP 56976 (taxotere): a semisynthetic analogue of taxol. J Natl Cancer Inst, *83:* 288-291, 1991.

19. Adams, J. The development of proteasome inhibitors as anticancer drugs. Cancer Cell, *5:* 417-421, 2004.

20. An, W. G., Hwang, S. G., Trepel, J. B., and Blagosklonny, M. V. Protease inhibitor-induced apoptosis: accumulation of wt p53, p21WAF1/CIP1, and induction of apoptosis are independent markers of proteasome inhibition. Leukemia, *14:* 1276-1283, 2000.

21. Nawrocki, S. T., Sweeney-Gotsch, B., Takamori, R., and McConkey, D. J. The proteasome inhibitor bortezomib enhances the activity of docetaxel in orthotopic human pancreatic tumor xenografts. Mol Cancer Ther, *3:* 59-70, 2004.

22. Huang, S., Pettaway, C. A., Uehara, H., Bucana, C. D., and Fidler, I. J. Blockade of NF-kappaB activity in human prostate cancer cells is associated with suppression of angiogenesis, invasion, and metastasis. Oncogene, *20:* 4188-4197, 2001.

23. Papandreou, C. N., Daliani, D. D., Nix, D., Yang, H., Madden, T., Wang, X., Pien, C. S., Millikan, R. E., Tu, S. M., Pagliaro, L., Kim, J., Adams, J., Elliott, P., Esseltine, D., Petrusich, A., Dieringer, P., Perez, C., and Logothetis, C. J. Phase I trial of the proteasome inhibitor bortezomib in patients with advanced solid tumors with observations in androgen-independent prostate cancer. J Clin Oncol, *22:* 2108-2121, 2004.

24. Petrylak, D. P. Chemotherapy for androgen-independent prostate cancer. Semin Urol Oncol, *20:* 31-35, 2002.

25. Pienta, K. J. and Smith, D. C. Paclitaxel, estramustine, and etoposide in the treatment of hormone-refractory prostate cancer. Semin Oncol, *24:* S15-72-S15-77, 1997.

26. Smith, D. C. and Pienta, K. J. Paclitaxel in the treatment of hormone-refractory prostate cancer. Semin Oncol, *26:* 109-111, 1999.

27. Khan, M. A., Carducci, M. A., and Partin, A. W. The evolving role of docetaxel in the management of androgen independent prostate cancer. J Urol, *170:* 1709-1716, 2003.

28. Logothetis, C. J. Docetaxel in the integrated management of prostate cancer. Current applications and future promise. Oncology (Huntingt), *16:* 63-72, 2002.

29. Obasaju, C. and Hudes, G. R. Paclitaxel and docetaxel in prostate cancer. Hematol Oncol Clin North Am, *15:* 525-545, 2001.

30. Dreicer, R., Magi-Galluzzi, C., Zhou, M., Rothaermel, J., Reuther, A., Ulchaker, J., Zippe, C., Fergany, A., and Klein, E. A. Phase II trial of neoadjuvant docetaxel before radical prostatectomy for locally advanced prostate cancer. Urology, *63:* 1138-1142, 2004.

31. Hussain, M., Smith, D. C., El-Rayes, B. F., Du, W., Vaishampayan, U., Fontana, J., Sakr, W., and Wood, D. Neoadjuvant docetaxel and estramustine chemotherapy in high-risk/locallyadvanced prostate cancer. Urology, *61:* 774-780, 2003.

32. Pettaway, C. A., Pisters, L. L., Troncoso, P., Slaton, J., Finn, L., Kamoi, K., and Logothetis, C. J. Neoadjuvant chemotherapy and hormonal therapy followed by radical prostatectomy: feasibility and preliminary results. J Clin Oncol, *18:* 1050-1057, 2000.

33. Herbst, R. S. and Khuri, F. R. Mode of action of docetaxel - a basis for combination with novel anticancer agents. Cancer Treat Rev, *29:* 407-415, 2003.

34. Herbst, R. S. and Langer, C. J. Epidermal growth factor receptors as a target for cancer treatment: the emerging role of IMC-C225 in the treatment of lung and head and neck cancers. Semin Oncol, *29:* 27-36, 2002.

35. Kuzur ME, A. K., Huntington MO, et al. A phase II trial of docetaxel and Herceptin in metastatic breast cancer patients overexpressing HER-2. Proceedings of the American Society of Clinical Oncology, *19:* 512, 2000.

36. Uber KA, N. B., Thor AD, etal. A phase II trial of weekly docetaxel (D) and herceptin (H) as first-or second-line treatment in HER-2 overexpressing metastatic breast cancer. Proceedings of the American Society of Clinical Oncology, *20:* 1949, 2001.

37. Esteva, F. J., Valero, V., Booser, D., Guerra, L. T., Murray, J. L., Pusztai, L., Cristofanilli, M., Arun, B., Esmaeli, B., Fritsche, H. A., Sneige, N., Smith, T. L., and Hortobagyi, G. N. Phase II study of weekly docetaxel and trastuzumab for patients with HER-2-overexpressing metastatic breast cancer. J Clin Oncol, *20:* 1800-1808, 2002.

38. Meden, H., Beneke, A., Hesse, T., Novophashenny, I., and Wischnewsky, M. Weekly intravenous recombinant humanized anti-P185HER2 monoclonal antibody (herceptin) plus docetaxel in patients with metastatic breast cancer: a pilot study. Anticancer Res, *21:* 1301-1305, 2001.

39. Piccart MJ, B. F., de Valeriola M, et al. A phase I, clinical and pharmacokinetic (PK) trial of the Farnesyl Transferase Inhibitor (FTI) R115777 + Docetaxel: a promising combination in patient (PTS) with solid tumors. Proceedings of the American Society of Clinical Oncology, *20:* 318, 2001.

40. Hayes DF, C. H., Marshall JL, Lippman D, Figuera M, Fingert H G3139 (oligonucleotide antisense against bcl-2) and docetaxel in patients with Bcl-2-positive malignancies. *In:* American Society of Clinical Oncology, 37th Annual Meeting; 12-15 May 2001, San Francisco, CA, USA, 2001.

41. Morris MJ, T. W., Cordon-cardo C, et al. BCL-2 antisense (G3139) plus docetaxel for treatment of progressive androgen-independent prostate cancer. European Journal of Cancer, *37:* 218, 2001.

42. Blagosklonny, M. V. Are p27 and p21 cytoplasmic oncoproteins? Cell Cycle, *1:* 391-393, 2002.

43. Coqueret, O. New roles for p21 and p27 cell-cycle inhibitors: a function for each cell compartment? Trends Cell Biol, *13:* 65-70, 2003.

44. Gartel, A. L. and Tyner, A. L. The role of the cyclin-dependent kinase inhibitor p21 in apoptosis. Mol Cancer Ther, *1:* 639-649, 2002.

45. Philipp-Staheli, J., Kim, K. H., Liggitt, D., Gurley, K. E., Longton, G., and Kemp, C. J. Distinct roles for p53, p27Kip1, and p21Cip1 during tumor development. Oncogene, *23:* 905-913, 2004.

46. Roninson, I. B. Oncogenic functions of tumour suppressor p21(Waf1/Cip1/Sdi1): association with cell senescence and tumour-promoting activities of stromal fibroblasts. Cancer Lett, *179:* 1-14, 2002.

Figure Legends

Figure 1. Effects of bortezomib and docetaxel on proliferation and apoptosis in the human prostate cancer cell line LNCaP-Pro5 *in vitro*, as measured by MTT assay and DNA fragmentation. **A**, effects of increasing dose bortezomib and steady dose docetaxel on proliferation. Cells were incubated with escalating doses of bortezomib alone or after exposure to docetaxel (10ng/mL) for 48 hours and analyzed by MTT analysis as described in Materials and Methods. Mean values presented are from eight replicate samples. Results of one experiment representative of three independent replicates. **B**, effects of increasing dose docetaxel and steady dose bortezomib on proliferation. Cells were incubated with escalating doses of docetaxel alone or after exposure to bortezomib (10nM) for 48 hours and analyzed by MTT analysis as described in Materials and Methods. Mean values presented are from eight replicate samples. Results of one experiment representative of three independent replicates. **C**, effects of increasing dose bortezomib and steady dose docetaxel on DNA fragmentation. Cells were incubated with escalating doses of bortezomib alone or after exposure to docetaxel (10ng/mL) for 48 hours and analyzed by propidium iodide staining and FACS analysis as described in Materials and Methods. *Columns,* mean (n=3); *bars,* SD. *, significantly different from control within the same treatment arm. **D**, effects of increasing dose docetaxel and steady dose bortezomib on DNA fragmentation. Cells were incubated with escalating doses of docetaxel alone or after exposure to bortezomib (10nM) for 48 hours and analyzed by propidium iodide staining and FACS analysis as described in Materials and Methods. *Columns,* mean (n=3); *bars,* SD. *, significantly different from control. **, significant

difference between docetaxel and bortezomib + docetaxel treatments. **E**, summary of effects of bortezomib and docetaxel on apoptosis. Cells were incubated with 10 nM bortezomib, 10 ng/mL docetaxel or bortezomib + docetaxel for 48 h. DNA fragmentation was measured by PI staining and FACS analysis as described in Materials and Methods. *Columns,* mean (n=3); *bars,* SD. *, significantly different from control. **, significant difference between docetaxel and bortezomib + docetaxel treatments.

Figure 2. Effects of docetaxel and known cell-cycle inhibitors on apoptosis as measured by DNA fragmentation *in vitro*. **A**, effects with roscovitine. Cells were incubated with 10 ng/mL docetaxel, 25 uM roscovitine or docetaxel + roscovitine for 48 h. DNA fragmentation was measured by PI staining and FACS analysis as described in Materials and Methods. **B**, effects with olomucine. Cells were incubated with 10 ng/mL docetaxel, 100 uM olomucine or docetaxel + olomucine for 48 h. DNA fragmentation was measured by PI staining and FACS analysis as described in Materials and Methods. *Columns,* mean (n=3); *bars,* SD. *, significantly different from control. **, significant difference between docetaxel and docetaxel + olomucine treatment.

Figure 3. Effects of bortezomib and docetaxel on p21 expression in the human prostate cancer cell line LNCaP-Pro5 *in vitro* as measured by immunoblotting. **A**, effects of bortezomib, docetaxel and the combination on apoptosis after 24 hours. Cells were incubated with 100 nM bortezomib, 100 ng/mL docetaxel or bortezomib + docetaxel for 24 h. DNA fragmentation was measured by PI staining and FACS analysis as described in Materials and Methods. *Columns,* mean (n=3); *bars,* SD. *, significantly different

from control. **, significant difference between docetaxel and bortezomib + docetaxel treatments. **B**, effects of bortezomib, docetaxel and the combination on p21 expression. Cells were incubated with 100 nM bortezomib, 100 ng/mL docetaxel or bortezomib + docetaxel for 24 h. Cells were harvested and lysed, and levels of p21 and actin were measured by immunoblotting. Results are representative of three independent replicates.

Figure 4. Effects of docetaxel and p21 transfection on apoptosis in the human prostate cancer cell line LNCaP Pro5 *in vitro*. **A**, effects of p21 transfection on apoptosis. Cells were transiently transfected with empty vector (control) or p21 cDNA for 48 h. as described in Materials and Methods. Cells were then incubated with the indicated concentrations of docetaxel for 48 h. DNA fragmentation was measured by PI staining and FACS analysis as described in Materials and Methods. *Columns,* mean (n=3); *bars,* SD. *, significantly different from control. **, significant difference between empty vector and p21 transfection treatments. **B**, confirmation of p21 transfection. Cells were transiently transfected with empty vector (control) or p21 cDNA for 48 h. as described in Materials and Methods. After another 48 h., cells were harvested and lysed, and levels of p21 were measured with immunoblotting. Results are representative of three independent replicates.

Figure 5. Effects of bortezomib and docetaxel on p21 expression in the human prostate cancer cell line LNCaP-Pro5 *in vitro* as measured by immunofluorescence. Cells were incubated with 100 nM bortezomib, 100 ng/mL docetaxel or bortezomib + docetaxel for 24 h. Levels of p21 were measured by immunofluorescence with FITC relative to

backround IgG levels and FACS analysis as described in Materials and Methods. Results are representative of three independent replicates. *Gates*, mean (n=3). *, significantly different from IgG control.

Figure 6. Effects of bortezomib and docetaxel within populations of p21 expressing (positive) and non-expressing (negative) cells on inducing apoptosis in the human prostate cancer cell line LNCaP-Pro5 *in vitro*, as measured by immunofluorescence and DNA fragmentation. **A**, DNA fragmentation peaks. Cells were incubated with 100 nM bortezomib, 100 ng/mL docetaxel or bortezomib + docetaxel for 24 h. Cells expressing p21 were identified by p21-FITC immunofluorescence as described in Materials and Methods. DNA fragmentation was measured by PI staining and FACS analysis for the total cell populations, the p21 positive cell populations and the p21 negative cell populations as described in Materials and Methods. Top row demonstrates cell sorting into populations of p21 positive cells (above gate) and p21 negative cells (below gate). Bottom three rows demonstrate DNA fragmentation peaks for each condition within the total, p21 positive, and p21 negative cell populations. **B**, summary of sub G0/G1 (apoptotic) peak data for the total, p21 positive and p21 negative cell populations. *Columns,* mean (n=3); *bars,* SD. *, significantly different from control. **, significant difference between docetaxel and bortezomib + docetaxel treatments. Note, the significant inhibition of apoptosis from combination therapy seen in the total cell population is absent in the p21 negative population.

Figure 7. Effects of silencing p21 and p27 on bortezomib inhibition of docetaxel-inducing apoptosis in the human prostate cancer cell line LNCaP-Pro5 *in vitro.* **A**, effects of silencing RNA. Cells were transfected with nonspecific (control), p21 or p27 silencing RNA for 48 hours as described in Materials and Methods. Cells were then incubated with 100 nM bortezomib, 100 ng/mL docetaxel or bortezomib + docetaxel for 24 hours. DNA fragmentation was measured by PI staining and FACS analysis as described in Materials and Methods. *Columns,* mean (n=3); *bars,* SD. *, significantly different from control. **, significant difference between docetaxel and bortezomib + docetaxel treatments. **B**, confirmation and effects of silencing RNA. Cells were transfected with nonspecific (control), p21 or p27 silencing RNA for 48 hours as described in Materials and Methods. After an additional 24 hours, cells were harvested and lysed, and levels of p21, p27 and actin were measured by immunoblotting. Results are representative of three independent replicates.

Fig. 1A

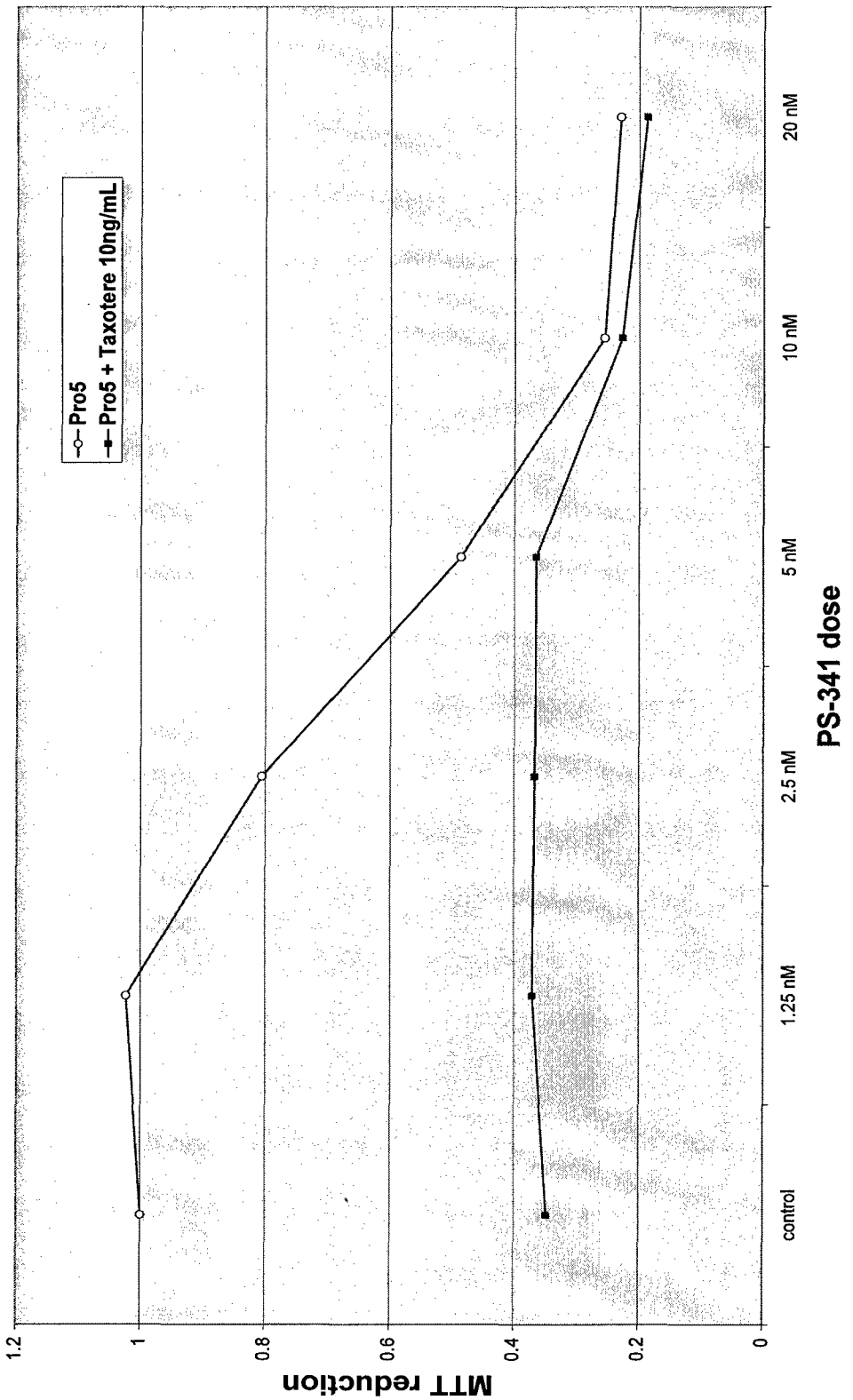
Pro5
Pro5 + Taxotere 10ng/mL
MTT reduction
1.2
1
0.8
0.6
0.4
0.2
0
control
1.25 nM
2.5 nM
5 nM
10 nM
20 nM
PS-341 dose

Fig. 1B

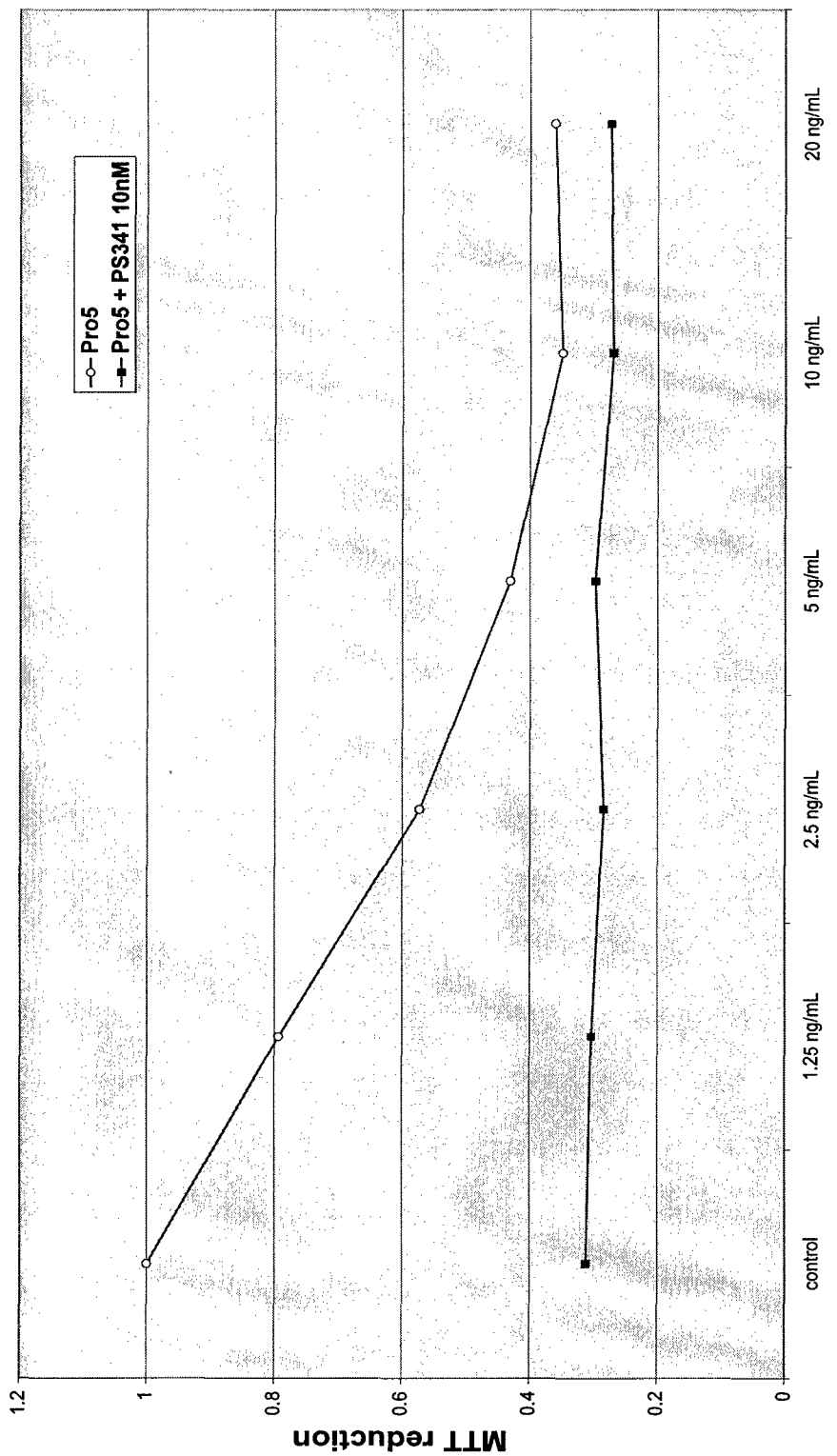
Pro5
Pro5 + PS341 10nM
MTT reduction
1.2
1
0.8
0.6
0.4
0.2
0
control
1.25 ng/mL
2.5 ng/mL
5 ng/mL
10 ng/mL
20 ng/mL
Taxotere dose

Fig. 1C

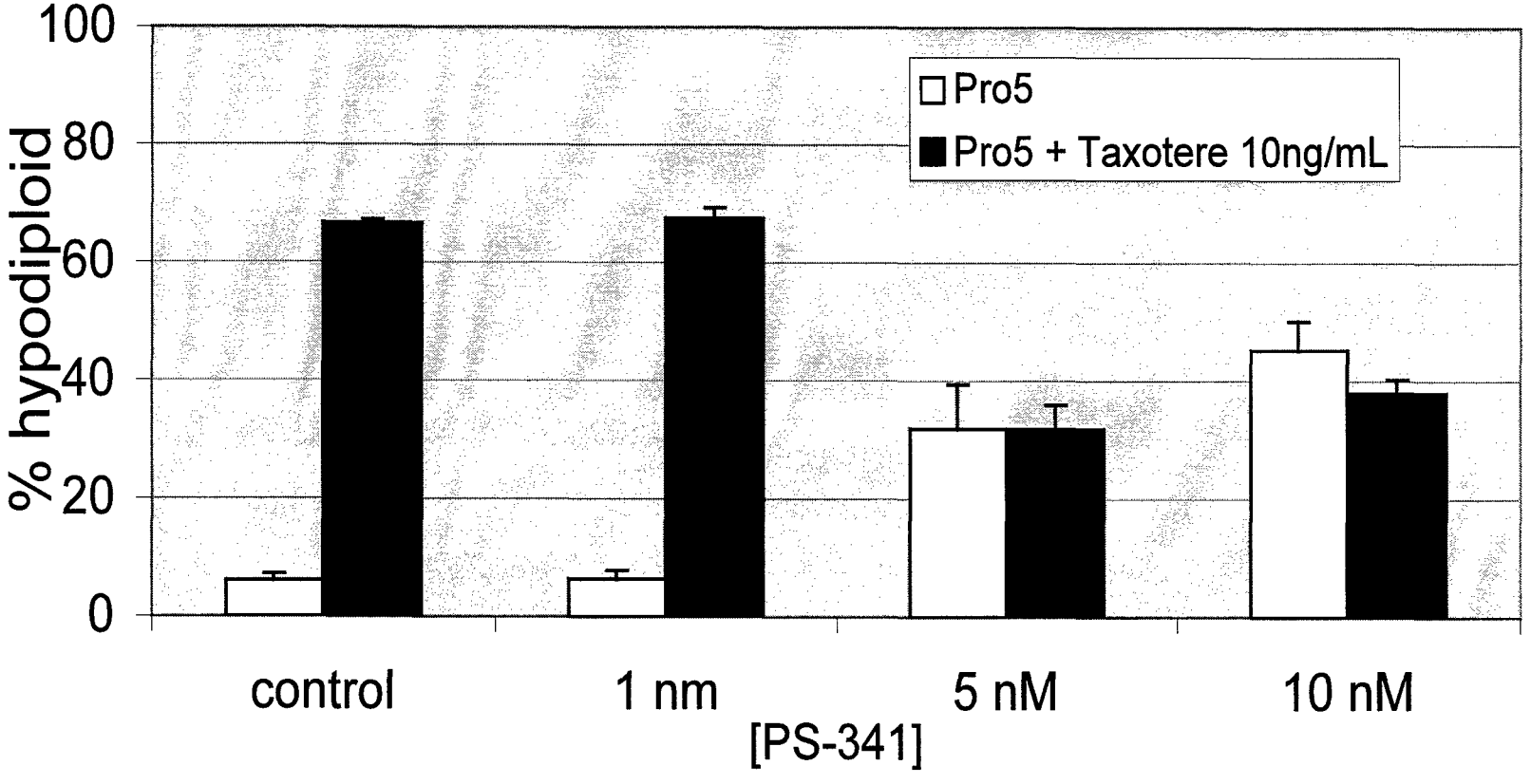
100
80
60
40
20
0
% hypodiploid
Pro5
Pro5 + Taxotere 10ng/mL
control
1 nm
5 nM
10 nM
[PS-341]

Fig. 1D

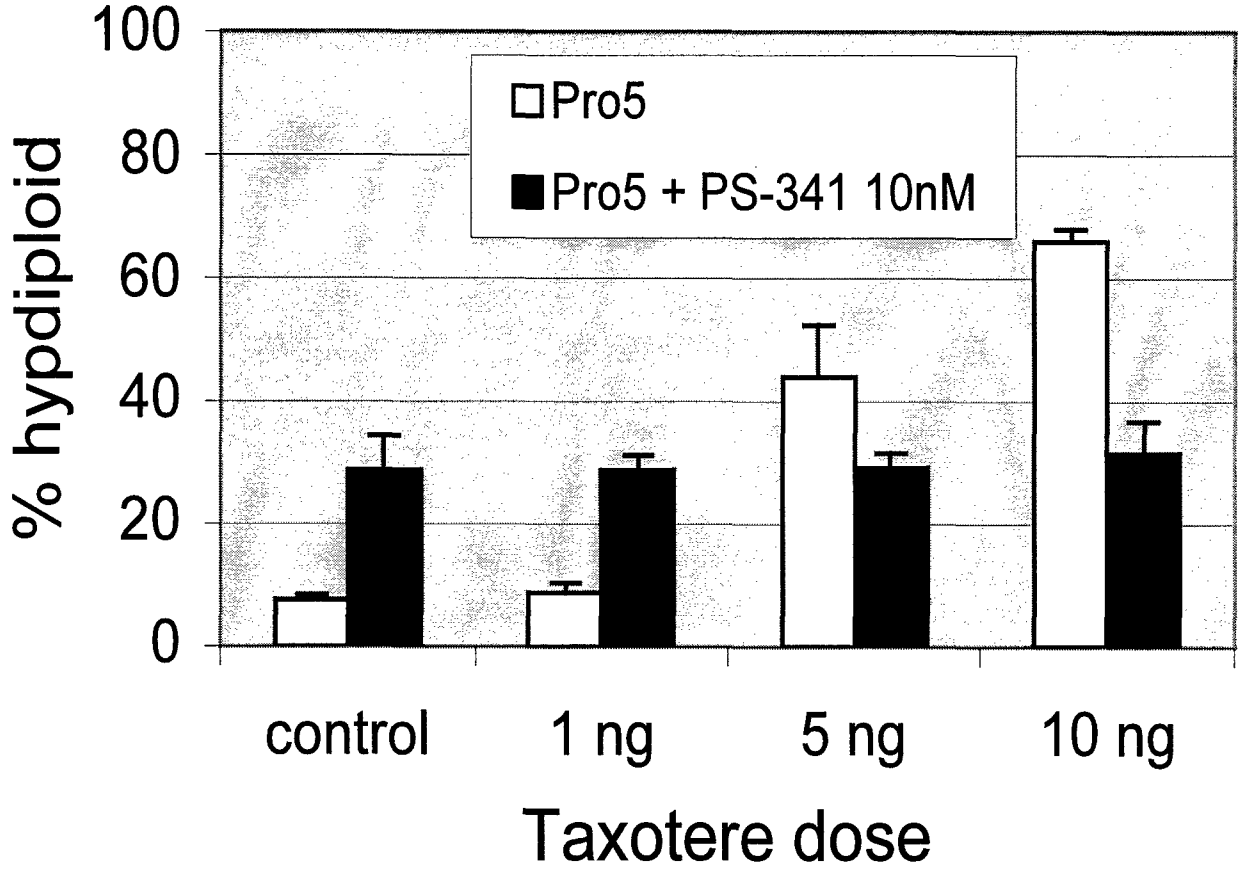
100
80
60
40
20
0
% hypdiploid
Pro5
Pro5 + PS-341 10nM
control
1 ng
5 ng
10 ng
Taxotere dose

Fig. 1E

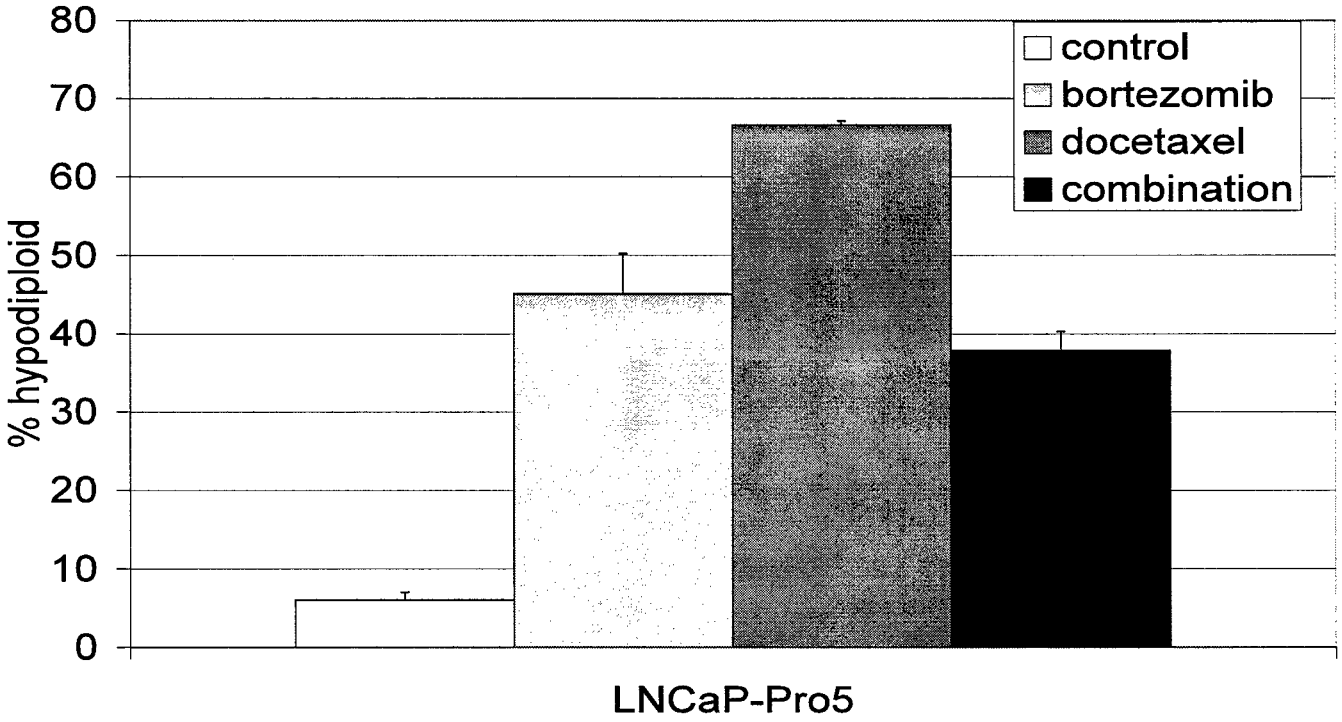
80
70
60
50
40
30
20
10
0
% hypodiploid
control
bortezomib
docetaxel
combination
LNCaP-Pro5

Fig. 2A

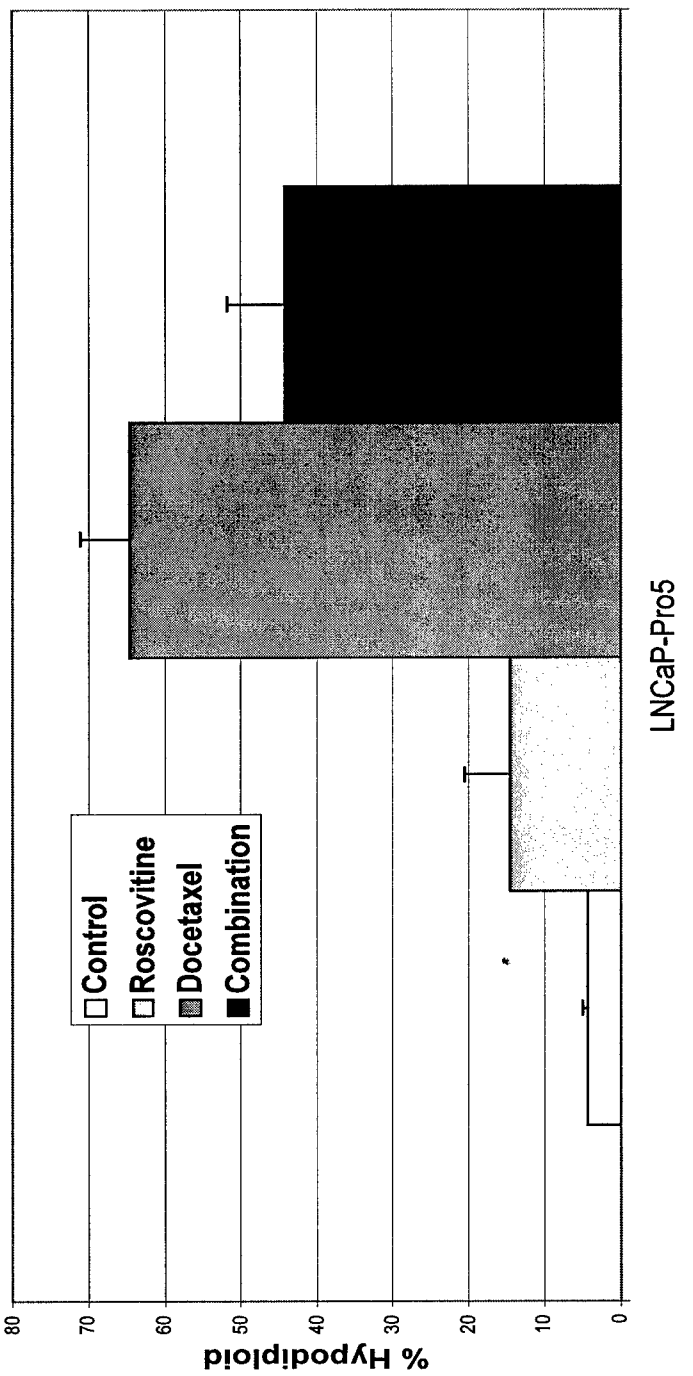
Control
Roscovitine
Docetaxel
Combination
% Hypodiploid
0
10
20
30
40
50
60
70
80
LNCaP-Pro5

Fig. 2B

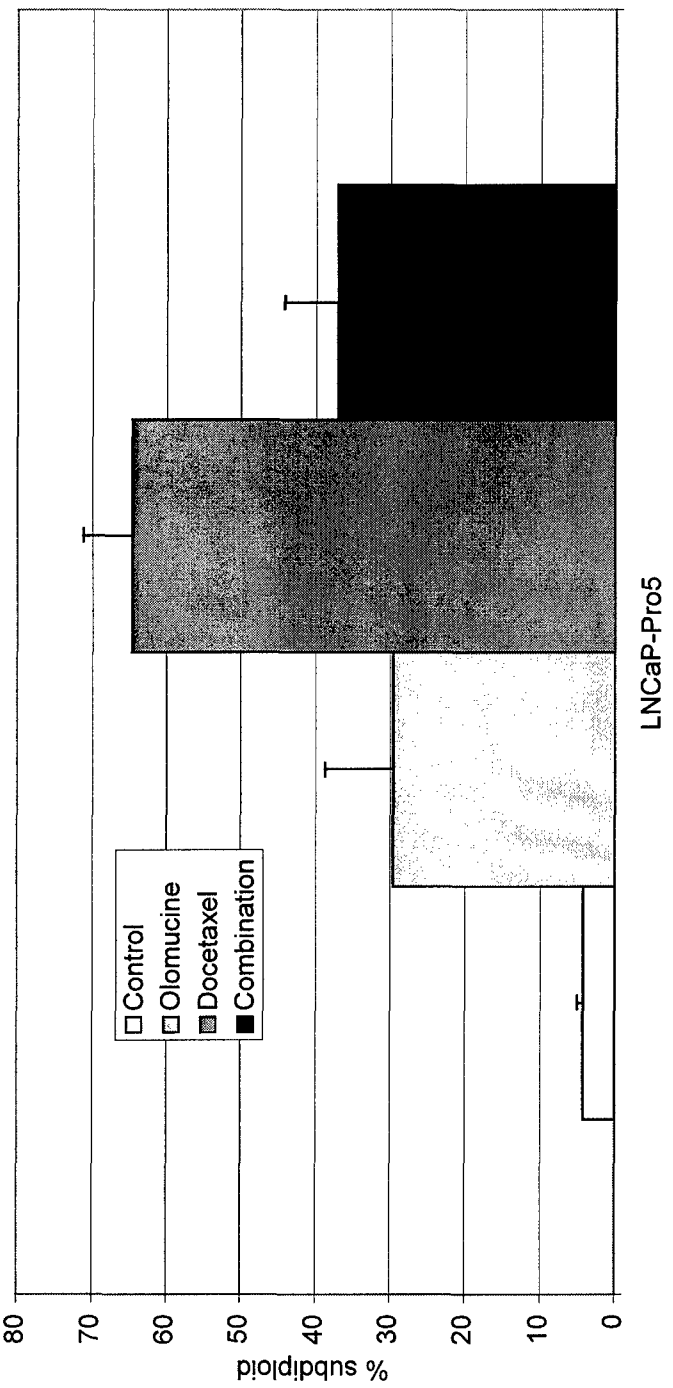
% subdiploid
0
10
20
30
40
50
60
70
80
Control
Olomucine
Docetaxel
Combination
LNCaP-Pro5

Fig. 3

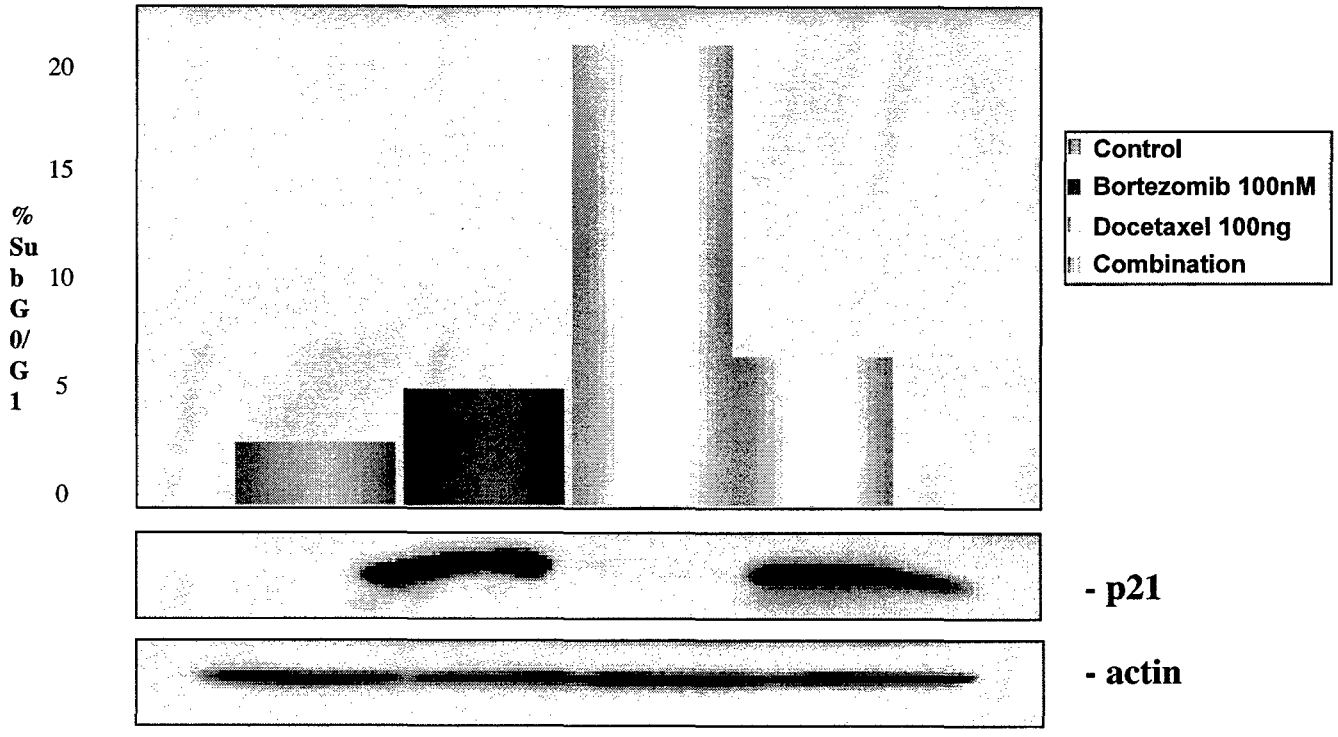
20
15
10
5
0
% Sub G0/G1
Control
Bortezomib 100nM
Docetaxel 100ng
Combination
- p21
- actin

Fig. 4

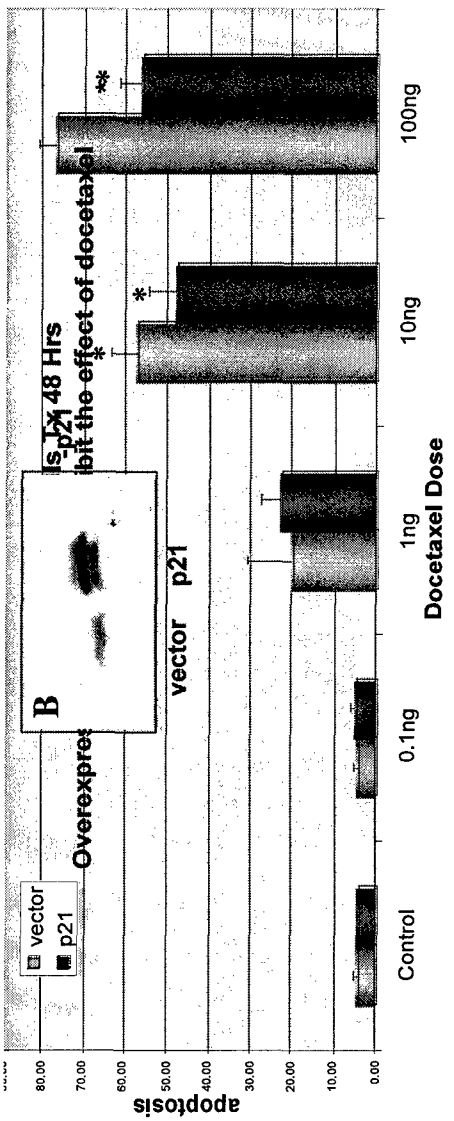
B
vector
p21
vector p21
apoptosis
80.00
70.00
60.00
50.00
40.00
30.00
20.00
10.00
0.00
Control
0.1ng
1ng
10ng
100ng
Docetaxel Dose
*
*
*
*

Fig. 5

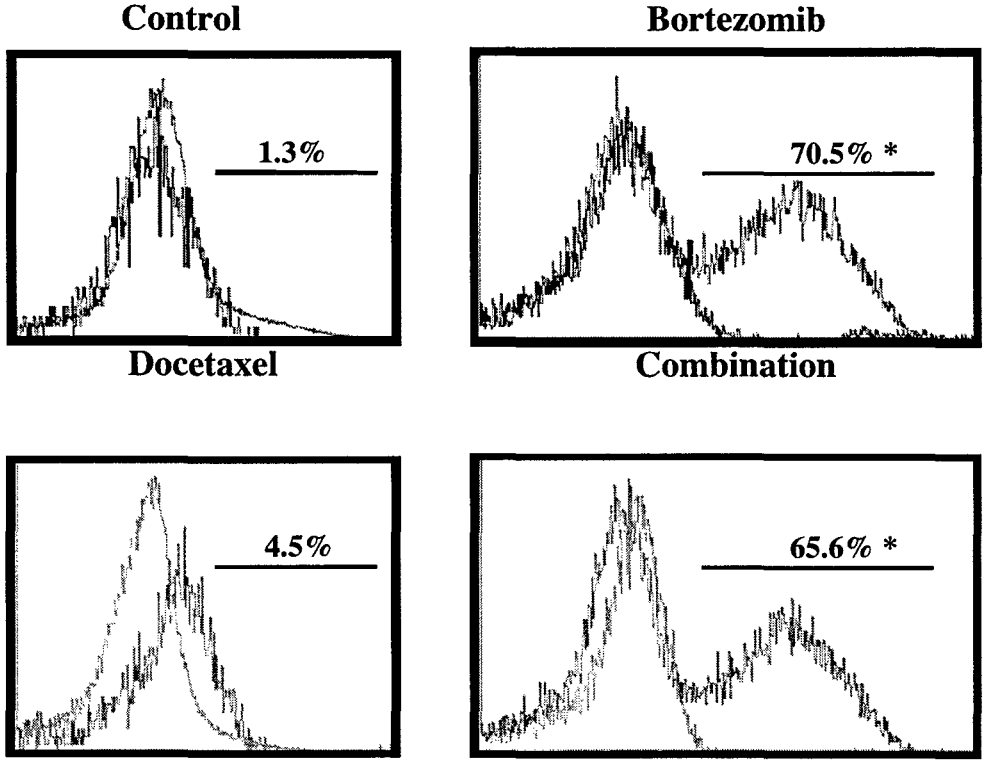

FITC IgG Isotype Control vs. p21

Fig. 6A

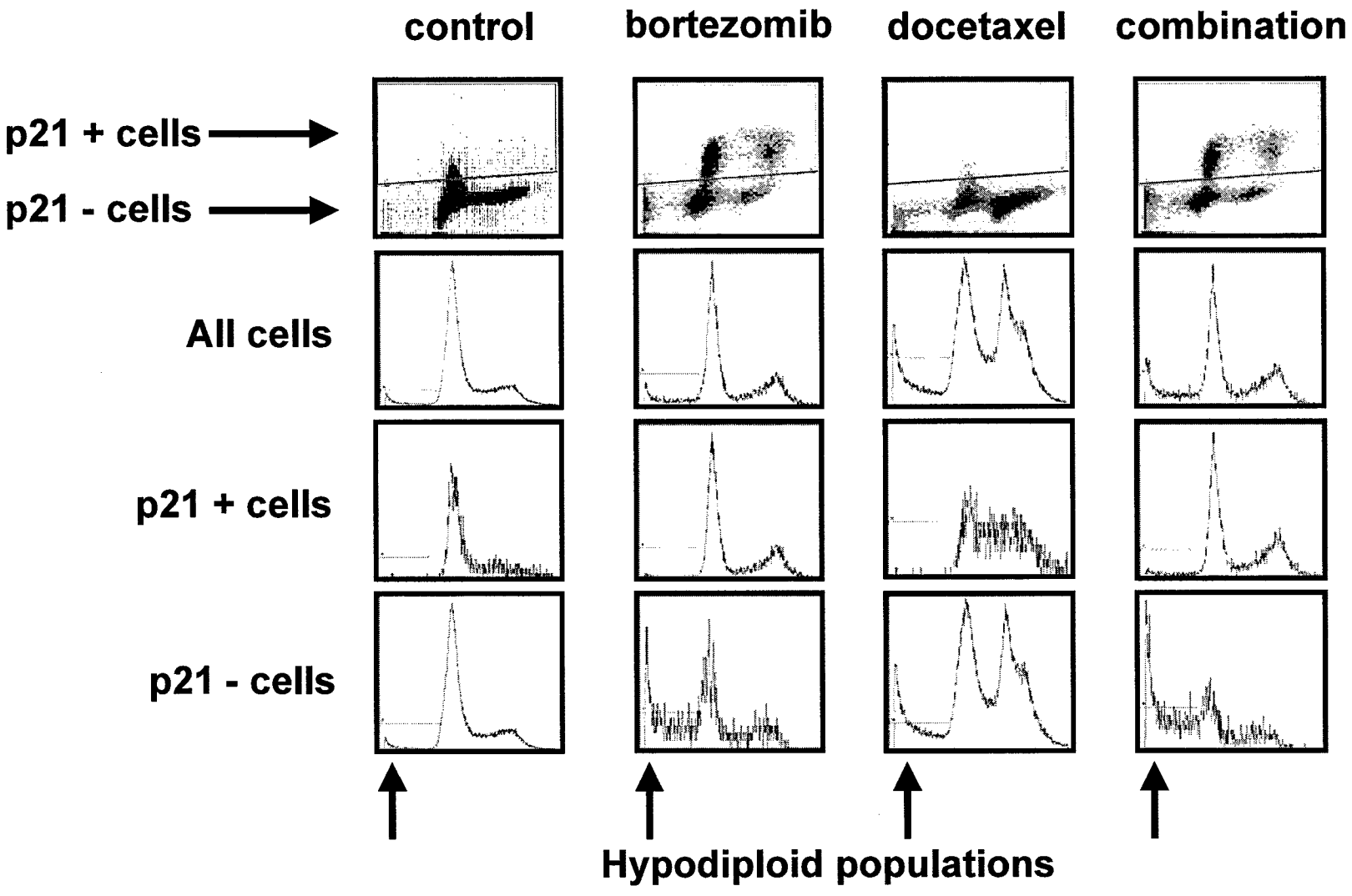
control
bortezomib
docetaxel
combination
p21 + cells
p21 - cells
All cells
p21 + cells
p21 - cells
Hypodiploid populations

Fig. 6B

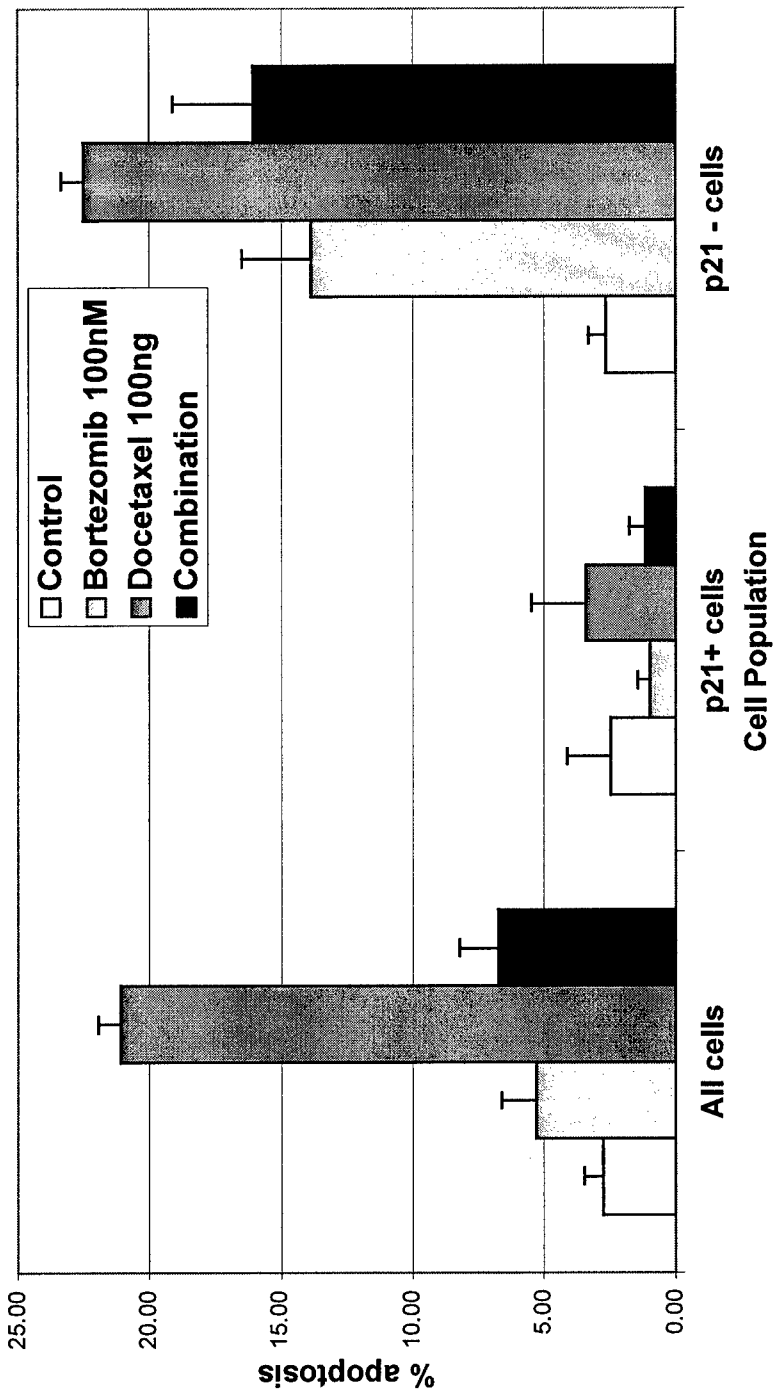
Control
Bortezomib 100nM
Docetaxel 100ng
Combination
25.00
20.00
15.00
10.00
5.00
0.00
% apoptosis
All cells
p21+ cells
p21 - cells
Cell Population

Fig. 7A

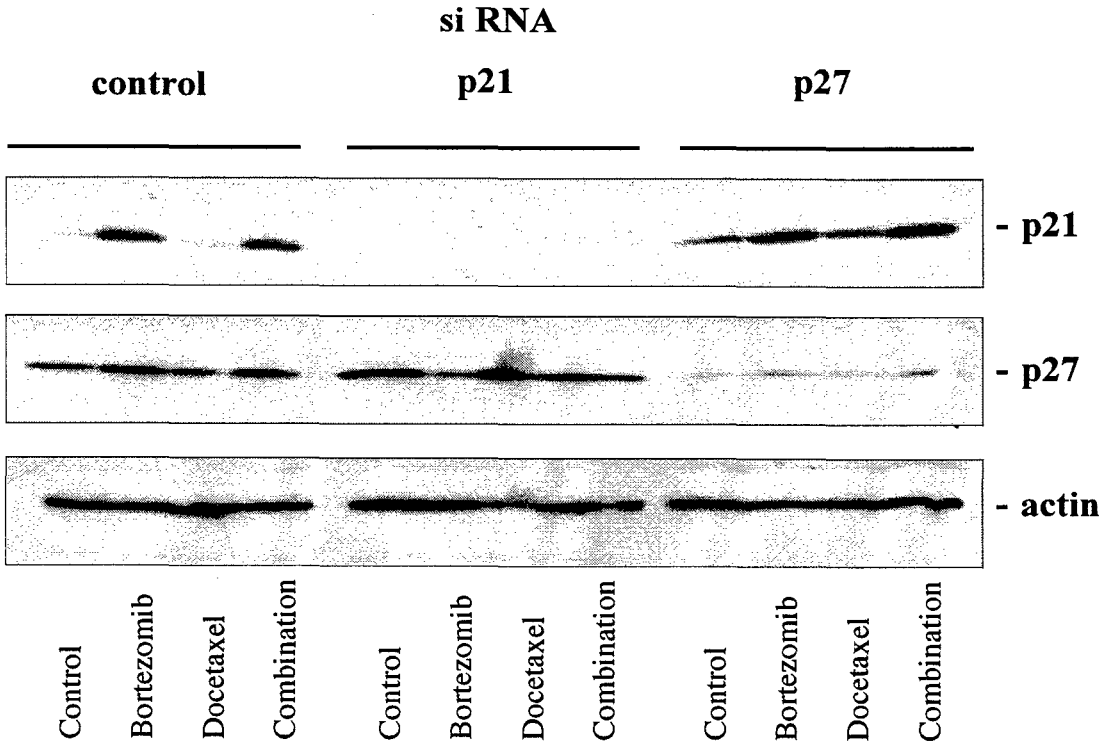
si RNA
control
p21
p27
- p21
- p27
- actin
Control
Bortezomib
Docetaxel
Combination
Control
Bortezomib
Docetaxel
Combination
Control
Bortezomib
Docetaxel
Combination

Fig. 7B

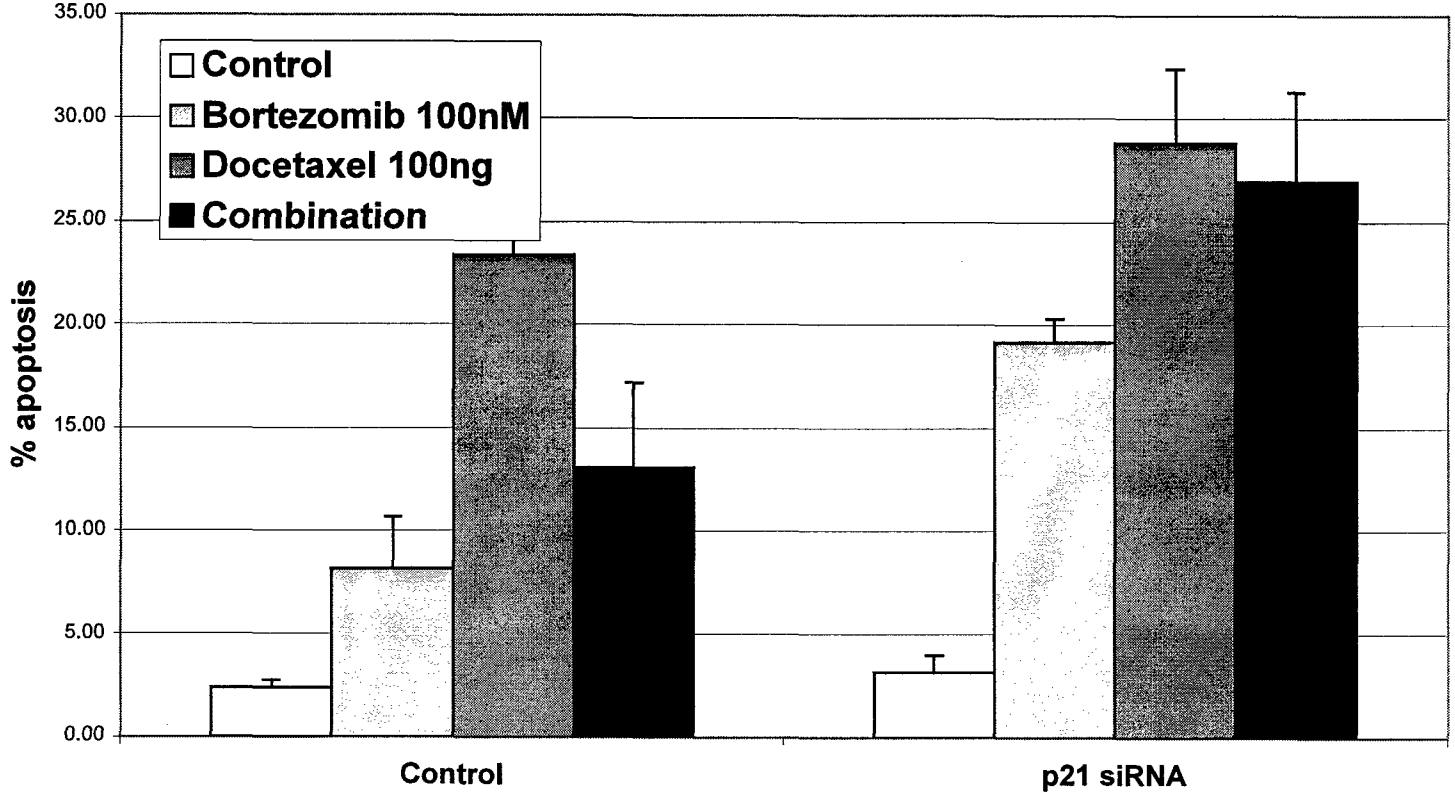
35.00
30.00
25.00
20.00
15.00
10.00
5.00
0.00
% apoptosis
Control
Bortezomib 100nM
Docetaxel 100ng
Combination
Control
p21 siRNA

Bortezomib abolishes TRAIL resistance via a p21-dependent mechanism in human bladder and prostate cancer cells.

Laura M. Lashinger[1], Keyi Zhu[1], Simon A. Williams[1], Marissa Shrader[1],

Colin P.N. Dinney[2], and David J. McConkey[1]

Departments of Cancer Biology[1] and Urology[2],

University of Texas M.D. Anderson Cancer Center,

Houston, Texas 77030

Running title: Apoptosis induced by TRAIL plus bortezomib

Key words: Proteasome inhibitor, Velcade, PS-341, caspase, cyclin-dependent kinase

Address correspondence to:
David McConkey
Department of Cancer Biology – 173
University of Texas M.D. Anderson Cancer Center
1515 Holcombe Boulevard
Houston, Texas 77030
Tel. (713) 792-8591
FAX (713) 792-8747
Email: dmcconke@mdanderson.org

FOOTNOTES

[3]Supported by a National Research Service Award (NRSA)(ZRG 1F0920)(to LML), the Department of Defense Prostate Cancer Research Program (W81XWH-04-1-0182)(to DJM), and the MD Anderson SPORE in Bladder Cancer (P50 CA91846)(to CPND and DJM).

[4]Abbreviations: BZ, bortezomib; cdk, cyclin-dependent kinase; DR, death receptor; FACS, fluorescence-activated cell sorting; FADD, Fas-associated death domain; FLIP, Flice-like inhibitory protein; HDAC, histone deacetylase; p21, $p21^{WAF\text{-}1/Cip\text{-}1}$, p27, $p27^{Kip\text{-}1}$; PI, propidium iodide; TBS-T, Tris-buffered saline with Tween-20; TNF, tumor necrosis factor; TRAIL, TNF-related apoptosis-inducing ligand.

ABSTRACT

TRAIL is a member of the TNF family of cytokines that induces apoptosis in some tumor cells but not in normal cells. Unfortunately, many human cancer cell lines are refractory to TRAIL-induced cell death, and the molecular mechanisms underlying resistance are unclear. Here we report that TRAIL resistance was reversed in human bladder and prostate cancer cell lines by the proteasome inhibitor bortezomib (PS-341, Velcade). Synergistic induction of apoptosis occurred within 4 to 6 hours in cells treated with TRAIL plus bortezomib and was associated with accumulation of $p21^{WAF-1/Cip-1}$ (p21) and inhibition of cyclin-dependent kinase activity. Roscovitine, a specific cyclin-dependent kinase 1/2 inhibitor, also sensitized cells to TRAIL. Silencing p21 expression reduced levels of DNA fragmentation by 50% in cells treated with bortezomib and TRAIL, confirming that p21 was required for the response. Analysis of the TRAIL pathway revealed that caspase 8 processing was enhanced in a p21-dependent fashion in cells exposed to TRAIL and bortezomib as compared to cells treated with TRAIL alone. As a result, all downstream components of the pathway (Bid cleavage, cytochrome c release and caspase 3 activation) were amplified. These data strongly suggest that p21-mediated cdk inhibition promotes TRAIL sensitivity via caspase-8 activation and that TRAIL and bortezomib should be combined in appropriate *in vivo* models as a possible approach to solid tumor therapy.

(219 words)

INTRODUCTION

Tumor necrosis factor (TNF)-related apoptosis-inducing ligand (TRAIL) is a homotrimeric cytokine that induces cell death in a variety of different cancer cell types but not in normal cells (1-3). TRAIL promotes apoptosis via binding to two surface receptors (DR4, DR5) that contain homologous death domains (DD) within their cytoplasmic tails, resulting in receptor trimerization and recruitment of the cytosolic death domain (DD)-containing protein, Fas-associated death domain (FADD) (4-7). This stimulated conformation of the TRAIL receptor, known as the death-inducing signaling complex (DISC) (8), allows FADD to recruit and activate procaspase 8, which then undergoes autocatalytic activation (9). Once fully activated, caspase 8 can either directly cleave and activate downstream effector caspases (3, 7) or it can stimulate a mitochondrial amplification loop by cleaving Bid, a BH3-only member of the Bcl-2 family (10-12). Studies in animal models indicate that systemic therapy with TRAIL is safe, and Phase I clinical trials designed to evaluate TRAIL toxicity and anti-tumor efficacy are being opened this year (13). However, *in vitro* data demonstrate that up to 50% of tumor cell lines do not undergo apoptosis in response to TRAIL. Thus, understanding the molecular mechanisms underlying TRAIL resistance and identifying strategies to reverse it are high priorities for ongoing research.

The 26S proteasome is a multicatalytic enzyme expressed in the nucleus and cytoplasm of all eukaryotic cells that degrades proteins targeted by ubiquitin conjugation (14). The proteasome is responsible for maintaining homeostasis by controlling intracellular levels of cell cycle regulatory proteins (p21, p27, and p53), transcription factors, and certain tumor suppressor genes/oncogenes, making it an attractive therapeutic

target in cancer (15-17). Bortezomib is a peptide boronate inhibitor of the proteasome that was developed as an anti-cancer agent several years ago and was the first such agent approved by the FDA for the treatment of a human cancer (multiple myeloma) (18). It selectively binds to and inhibits the chymotryptic-like activity of the proteasome at nanomolar concentrations, and in National Cancer Institute's 60 cancer cell line screen, bortezomib displayed a mean IC_{50} of 7nM with a unique spectrum of anticancer activity (19). Cellular responses depend on tumor type and range from cell cycle inhibition to apoptosis, and *in vivo* studies have demonstrated that bortezomib inhibits the growth of a variety of different solid tumors without significant toxicity (19-23).

Here we report that TRAIL-resistant human prostate and bladder cancer cell lines can be rapidly sensitized to TRAIL-induced apoptosis by treating them with bortezomib. The molecular mechanisms underlying the effects of bortezomib involve p21 accumulation and enhanced activation of caspases 8 and 3.

MATERIALS AND METHODS

Cell Culture and Reagents The LNCaP-derived cell line, LNCaP-Pro5 (24), was generously provided by Dr. Curtis Pettaway, Department of Urology, MD Anderson Cancer Center. The 253J B-V cells were derived from the 253J parental line by orthotopic "recycling" through the mouse bladder as described previously (25). The UM-UC3 cells were obtained from H. Barton Grossman, Department of Urology, U.T. M.D. Anderson Cancer center. Human PC-3 and DU-145 prostate cancer cells were obtained from American Type Culture Collection (ATCC, Rockville, MD). The prostate cancer cells were grown in RPMI-1640 (Life Technologies, Inc.) supplemented with 10% fetal

bovine serum (Life Technologies, Inc.) and 1% MEM vitamin solution (Life Technologies, Inc.), sodium pyruvate (BioWhittaker), L-glutamine (BioWhittaker), penicillin/streptomycin solution (BioWhittaker), and nonessential amino acids (Life Technologies, Inc.) under an atmosphere of 5% CO_2 in an incubator. The bladder cancer cells were cultured in MEM medium containing the same supplements. Bortezomib was kindly supplied by Millenium Pharmaceuticals (Cambridge, MA), and rhTRAIL was purchased from R&D Systems, Inc., Minneapolis, MN).

Quantification of apoptosis by PI/FACS Cells were treated with 10ng/mL of rhTRAIL and/or 100nM bortezomib for the times indicated. Both growth and wash media were saved and cells were harvested with trypsin. Supernatants were removed and pellets were resuspended in 400 μL of propidium iodide (PI) solution (50μg/mL propidium iodide, 0.1% Triton X-100, and 0.1% sodium citrate in PBS). Samples were then incubated overnight at 4°C in the dark before analysis by flow cytometry. The cells with sub-diploid DNA content were quantified to determine the percentage of cells containing apoptotic, fragmented DNA (26).

Quantitative analysis of phosphatidylserine exposure. Cells were treated with 10ng/mL of rhTRAIL and/or 100nM bortezomib for the times indicated prior to harvest with trypsin. Exposure of phosphatidylserine was measured by annexin V binding as described previously (27) using a commercial kit (Annexin V-PE Apoptosis Detection kit, BD Biosciences, San Diego, CA) according to manufacturer's protocol. Cell pellets were washed twice with cold PBS and resuspended in 1x binding buffer (10 mM

Hepes/NaOH (pH 7.4), 140 mM NaCl, 2.5 mM $CaCl_2$) at a concentration of 1 x 10^6 cells/mL. Aliquots of 100 μL were transferred to separate tubes and 5 μL of Annexin V-PE plus 5 μL of 7-AAD (7-Amino-actinomycin D) were added to each. After vortexing, cells were incubated at room temperature for 15 minutes in the dark. Samples were dilited with 400 μl of 1x binding buffer, and surface annexin-V immunofluorescence was quantified immediately by flow cytometry.

Immunoblot analyses. Cells were lysed by incubation for 1h at 4°C in 100μL of Triton lysis buffer [1% Triton X-100, 150mM NaCl, 25mM Tris (pH 7.5), 1mM glycerol phosphate, 1mM sodium orthovanadate, 1mM sodium fluoride, and 1 Complete Mini Protease Inhibitor Cocktail tablet (Roche, Indianapolis, IN)]. Lysates were centrifuged for 5 min at 12,000 x g (4°C), and 20 μg of the postnuclear supernatants were mixed with equal volumes of 2x SDS-PAGE sample buffer (50mM Tris-HCl, 2% SDS, 0.1% bromophenol blue, 10% glycerol, and 5% β-mercaptoethanol). Samples were then boiled, for 5 minutes at 100°C and resolved by 15% SDS-PAGE at 100V for 90 min. Polypeptides were transferred to nitrocellulose membranes for 90 min at 100V in a transfer buffer containing 39mM glycine, 48mM Tris, and 20% methanol. Membranes were blocked for 1 hr in 5% milk diluted in Tris-buffered saline containing 0.1% Tween-20 (TBS-T). Membranes were incubated overnight at 4°C with primary antibodies specific for caspase 8 [(Cell Signaling Technology, Beverly, MA), 1:1000 dilution], caspase 3, cytochrome-c, p21, or p27 [Pharmingen, San Diego, CA 1:1000 dilution], or Bid [(R&D Biosystems, Minneapolis, MN), 1:1000 dilution]. Blots were washed 3 x 5 min in TBS-T before incubation with secondary antibodies [horseradish peroxidase-

conjugared sheep antimouse or donkey anti-rabbit antibody (Amersham Biosciences, Piscataway, NJ), 1:1000 dilution] for 2h at 4°C. Blots were washed 3X 10 min in TBS-T and developed by enhanced chemiluminescence (Renaissance; New England Nuclear, Boston, MA).

Caspase 3 Assay Cells were treated with 100nM bortezomib and/or 10ng/mL rhTRAIL for the times indicated and harvested with trypsin. Growth and wash media were saved and cell pellets were washed once with PBS. Supernatants were removed and pellets were lysed with 200μL cold lysis buffer (100 mM HEPES (pH 7.4), 1% sucrose, 0.1% CHAPS, 1 mM EDTA, 100 mM DTT) containing a protease inhibitor cocktail ("Complete Mini" Protease Inhibitor Tablet, Boehringer, Indianapolis, IN). Cells were lysed at 4°C for 1 hr and centrifuged, and 800μL of caspase buffer plus 2μL of 20 mM DEVD-AFC fluorogenic substrate (AFC 138, Enzyme Systems Products, Livermore, CA) was added to each supernatant. Samples were incubated for 1hr at 37°C in the dark and diluted with 1 mL caspase buffer, and released AFC fluorescence was quantified using a Shimadzu spectrofluorimeter (Model RF-1501).

Immune complex cdk2 kinase assays Cells were cultured to 60% confluency in 10 cm dishes and treated with various concentrations of bortezomib or roscovitine for 24 hours. Cells were then harvested with trypsin and lysed by rotating them for 1 h at 4° C in 1mL of the Triton X-100 lysis buffer described above. Lysates were cleared by centrifugation for 10 min at 12,000 x g (4°C). Supernatants containing 400 μg of protein were then incubated with an anti-cdk2 antibody for 2 hr followed by overnight incubation with 50

μL protein A/G-Sepharose beads (Santa Cruz Biotechnology, Santa Cruz, CA) at 4°C. The beads were then washed twice with lysis buffer and twice more with kinase buffer (25 mM Tris, pH 7.2, and 10 mM $MgCl_2$). Immunoprecipitates were incubated with 1 μg histone H1, 150 μM ATP, and 20 μCi [γ-^{32}P] ATP in 50 μL of kinase buffer for 15 min at 30°C. SDS sample buffer was used to terminate the reaction and the mixture was boiled for 5 min at 100°C. Finally, the mixture was loaded onto 12% SDS-PAGE gels and resolved at 100V for 90 min. The gels were stained with Coomassie blue, destained, dried, and analyzed by autoradiography.

siRNA-mediated silencing of p21. Cells were grown to 60% confluency in 6-well plates and transfected with specific or non-specific siRNA constructs for 48 hours according to the manufacturer's protocols. The constructs utilized were the siRNA SMARTpool cdk-N-1A ($p21^{WAF-1/Cip-1}$) and cdk-N-1B ($p27^{Kip-1}$)(Upstate Cell Signaling Solutions; Lake Placid, NY) or the siRNA Nonspecific Control IV (DHARMACON RNA Technologies, Lafayette, CO), all at 200 nM. Liposome-mediated transfection was accomplished with Oligofectamine Reagent (Invitrogen Life Technologies; Carlsbad, CA) diluted 1:100 in serum-free MEM. Following silencing cells were treated with rhTRAIL (10ng/mL) and bortezomib (100nM) for 8 hours and DNA fragmentation was quantified by PI/FACS. The efficiency of p21 or p27 silencing was verified in each experiment by immunoblotting.

RESULTS

Effects of bortezomib on TRAIL-induced apoptosis. Previous studies have implicated the NFκB pathway in the regulation of TRAIL resistance (28, 29). In preliminary experiments, we found that many human bladder and prostate cancer cell lines are refractory to TRAIL-induced apoptosis at baseline. Hypothesizing that NFκB activation maintains the resistant phenotype in these cell lines, we treated them simultaneously with TRAIL plus bortezomib (a potent NFκB antagonist)(30) and measured DNA fragmentation by PI/FACS analysis 24 hours later. The results revealed a dramatic synergistic interaction between bortezomib and TRAIL in all of the cell lines (Fig. 1A). We confirmed these results using an independent measure of apoptosis (Annexin-V staining) for detection of phosphatidylserine externalization (Fig. 1B). In contrast, a more selective inhibitor of NFκB (the IKK antagonist PS-1145) (31) had no effect on TRAIL-induced apoptosis (Fig. 1C), strongly suggesting that NFκB inhibition did not account for the effects of bortezomib on TRAIL sensitivity.

In subsequent experiments we characterized the effects of bortezomib on critical components of the TRAIL cell death pathway. Kinetic analyses demonstrated that TRAIL sensitization occurred as early as 4-6 hrs in the LNCaP Pro5 and 253JB-V cells (60.0 ± 8.56, $p<0.001$ and 60.8 ± 10.5, $p<0.001$, respectively) (Fig 2A). Immunoblotting studies demonstrated that bortezomib had no effect on proteolytic processing and activation of caspase-8, whereas incubation with TRAIL resulted in partial proteolytic processing of caspase-8 to form a 43/41kDa intermediate by 8 hours (Fig 2B). In cells treated with bortezomib plus TRAIL, this intermediate formed with much more rapid

kinetics (<30 min), and it was accompanied by the formation of a smaller fragment (18kDa) characteristic of the active, large subunit of caspase-8 (Fig. 2B). Cells treated with TRAIL plus bortezomib in the presence of a caspase-8-selective peptide antagonist, IETDfmk (10 μM), displayed no DNA fragmentation above controls (data not shown), consistent with previous studies that demonstrated that caspase-8 is required for TRAIL-induced cell death (32). Cells treated with TRAIL plus bortezomib also displayed enhanced cleavage of Bid and release of cytochrome c (Fig. 2C). Finally, exposure to either bortezomib or TRAIL alone had little effect on procaspase-3, whereas treatment with the combination promoted rapid proteolytic processing of procaspase-3 and its enzymatic activation (Fig 2D). Together, these data demonstrate that bortezomib interacts with the TRAIL pathway at the level of caspase-8 to promote the initiation of mitochondrial events (cytochrome c release) that dramatically amplify caspase-3 activation. These effects probably account for the synergistic induction of DNA fragmentation and phosphatidylserine exposure observed in cells treated with the combination.

Role of p21 in bortezomib-induced TRAIL sensitization. Although treatment with bortezomib alone failed to induce significant increases in apoptosis in the tested cell lines, previous work from our laboratory demonstrated that it blocks DNA synthesis at low nanomolar concentrations in bladder cancer cells irrespective of whether or not it induces cell death (33). The effects on DNA synthesis are associated with accumulation of cyclin-dependent kinase inhibitors, p21 and p27, and inhibition of cdk2 and cdc2 activity (30, 33, 34). Furthermore, p21 accumulation is considered a marker for effective inhibition of the proteasome (35). Consistent with the previous studies, bortezomib

induced a time-dependent accumulation of p21 in all of the TRAIL-resistant cells examined here (Fig. 3A and data not shown). Bortezomib also stimulated increases in p27 expression with similar kinetics (Fig. 4B and data not shown). Immune complex kinase assays confirmed that accumulation of p21 and p27 was associated with inhibition of cdk2 activity (Fig. 2B).

To determine whether or not cdk inhibition was sufficient to promote TRAIL sensitization, we examined the effects of the broad-spectrum cdk inhibitor, roscovitine, on TRAIL-induced apoptosis. Roscovitine had no effect on apoptosis at the concentration and time point studied in the 253J B-V cells but did induce DNA fragmentation in LNCaP-Pro5 cells (Fig. 3C). Combined treatment with roscovitine plus TRAIL resulted in synergistic induction of DNA fragmentation in both cell lines as measured by PI/FACS (Fig. 2C). Similar results were obtained with another, structurally unrelated cdk inhibitor (olomoucine) but not with an inactive structural analog of the compound (iso-olomoucine)(data not shown). Together, these results suggest that inhibition of cdk activation is sufficient to explain the effects of bortezomib on TRAIL sensitization. However, cdk inhibitors (i.e., flavopiridol) can also interfere with transcription (36, 37), and these off-target effects may contribute to the TRAIL sensitization observed in cells treated with roscovitine or olomoucine as well.

To more directly assess the involvement of p21 and p27 in bortzomib-mediated TRAIL sensitization, we compared the levels of DNA fragmentation observed in LNCaP-Pro5 cells exposed to a control siRNA construct to those observed in LNCaP-Pro5 cells exposed to siRNA specific for p21 or p27. Immunoblotting confirmed that silencing was efficient in cells exposed to either of the specific constructs but not in the controls (Figs.

4A,B). Levels of DNA fragmentation in the p21-silenced cells were significantly lower than those observed in controls (32% versus 66%, or a 50% reduction, $p < 0.001$), confirming that the bortezomib-induced accumulation of p21 contributed directly to TRAIL sensitization. Levels in the p27-silenced cells also appeared to be consistently lower than in controls (Fig. 4B), but the effects did not reach statistical significance, and our attempts to simultaneously silence both p21 and p27 were unsuccessful. Silencing p21 inhibited procaspase-8 activation as measured by immunoblotting (Fig. 4C) or using a fluorigenic caspase-8 peptide substrate (data not shown), demonstrating that p21 acted at the level of procaspase-8 to promote cell death. As a result, processing of procaspase-3 was also reduced in cells depleted of p21 (Fig. 4C).

DISCUSSION

Bortezomib and TRAIL are undergoing evaluation in clinical trials in a variety of different malignancies. Here we report that they can be combined to induce synergistic cell death in genitourinary cancer cells in vitro and in vivo. Characterization of the molecular mechanisms involved link the effects of bortezomib to increased caspase-8 activation, indicating that the drug affects TRAIL sensitivity at one of the earliest steps in the pathway. Cell death occurred with strikingly rapid kinetics (4-8 h) as compared to responses to single or combined conventional chemotherapeutic agents, which in our hands require 24-48 h in these cells. In fact, the kinetics of cell death observed here were more rapid than any we have observed in a solid tumor model exposed to any agent, including pharmacological agents (staurosporine, thapsigargin) that are considered the most potent triggers of cell death.

The transcription factor NFκB has received considerable attention for its role in cancer cell survival pathways (38). Bortezomib is a potent inhibitor of NFκB activation via stabilization of NFκB's physiological inhibitor, IκBα, and its effects as an NFκB inhibitor have been used to sensitize cancer cells to other death stimuli (38). Although inhibition of NFκB was an attractive explanation for bortezomib's effects on TRAIL sensitivity, we were unable to mimic them with a more specific inhibitor of the pathway (the IKK inhibitor PS-1145). Rather, TRAIL sensitization was associated with the accumulation of p21 and inhibition of cdk2 activity, and it was reversed in cells transfected with an siRNA construct specific for p21. Although it is possible that p21 promotes TRAIL sensitivity via a direct mechanism, the observation that chemical cdk inhibitors like roscovitine (Fig. 3C) (39) and flavopiridol (40-42) can also synergistically

sensitize cells to TRAIL strongly suggests that p21's effects are mediated by cdk inhibition. Based on these results, we would predict that any stimulus that directly or indirectly causes cdk inhibition would sensitize cancer cells to TRAIL-mediated cell death. Support for this concept comes from the observation that tumor cells are most sensitive to TRAIL in the G1 phase of the cell cycle (43), and DNA damaging agents synergize with TRAIL to promote apoptosis in cells that retain wild-type p53 (44), where p53-mediated p21 expression and cell cycle arrest should occur. Accumulation of p21 also underlies TRAIL sensitization induced by resveratrol (45) and probably contributes to the synergistic increases in apoptosis observed in cells treated with TRAIL plus histone deacetylase (HDAC) inhibitors (46, 47).

Although our data suggest that p21-mediated cdk inhibition is responsible for the increased caspase-8 activation observed in cells treated with bortezomib plus TRAIL, further study is required to elucidate the specific mechanisms involved. One issue is our observation that enhanced caspase-8 processing was detected as early as 30 min after treatment with TRAIL plus bortezomib, which was somewhat faster than the kinetics of p21 accumulation measured by immunoblotting. This observation coupled with the incomplete suppression of DNA fragmentation observed in the p21- or p27-silenced cells suggest that additional bortezomib-sensitive mechanism(s) are involved. Studies in other models concluded that bortezomib enhanced surface DR5 expression (48) and decreased levels of c-FLIP (48, 49), both of which could contribute to the increased caspase-8 activation observed. We have confirmed that bortezomib and roscovitine increase surface DR5 expression in the LNCaP-Pro5 and 253J B-V cells, but their effects are delayed (>12 h) relative to the rapid kinetics of caspase activation and DNA

fragmentation (4-8 h)(L. Lashinger, M. Shrader, unpublished observations). We also investigated the effects of bortezomib on expression of c-FLIP and the TRAIL decoy receptors (DcR-1, and DcR-2) in our cells and did not detect any obvious changes that might account for the phenomenon (L. Lashinger, unpublished observations). On the other hand, the FADD adaptor protein is known to be phosphorylated in a cell cycle-sensitive manner (50-52), and in preliminary studies we have found that combined treatment with bortezomib plus TRAIL leads to changes in FADD phosphorylation that are not observed in response to treatment with either agent alone (S. Williams, unpublished observations). Therefore, in ongoing studies we are attempting to define the potential biological significance of these changes in FADD phosphorylation in our cell lines.

Accumulating evidence indicates that cell cycle progression and cell death are mechanistically inter-related (53). Specifically, alterations that promote cell cycle progression often sensitize cells to death, whereas processes that inhibit cell cycle progression block cell death (53). Most of the investigational agents being studied at present (i.e., growth factor receptor antagonists, kinase inhibitors, HDAC inhibitors, bortezomib, etc) arrest cells in G_1 (54), which may enable them to reinforce the growth inhibitory/cytostatic effects of conventional chemotherapy but probably does not make them particularly effective in promoting cell killing. Coupled with the other studies described above, our data strongly suggest that cell cycle arrest at the G_1/S checkpoint promotes sensitivity to TRAIL-mediated apoptosis in cancer cells, which places it in a unique category relative to other death-inducing stimuli. Thus, TRAIL –based combination therapy appears to be qualitatively different from other combinations of

biological and cytotoxic agents because it is most active in cells that have been growth arrested. The data provide a compelling rationale for performing more extensive studies to optimize the anti-tumor activities of these combinations in appropriate preclinical models in preparation for clinical studies in patients. Our preliminary studies (L. Lashinger, unpublished observations) indicate that biologically active doses of bortezomib and recombinant human TRAIL can be delivered to nude mice without generating systemic toxicity.

REFERENCES

1. Wiley, S. R., Schooley, K., Smolak, P. J., Din, W. S., Huang, C. P., Nicholl, J. K., Sutherland, G. R., Smith, T. D., Rauch, C., Smith, C. A., and et al. Identification and characterization of a new member of the TNF family that induces apoptosis. Immunity, *3:* 673-682, 1995.
2. Walczak, H., Miller, R. E., Ariail, K., Gliniak, B., Griffith, T. S., Kubin, M., Chin, W., Jones, J., Woodward, A., Le, T., Smith, C., Smolak, P., Goodwin, R. G., Rauch, C. T., Schuh, J. C., and Lynch, D. H. Tumoricidal activity of tumor necrosis factor-related apoptosis-inducing ligand in vivo. Nat Med, *5:* 157-163, 1999.
3. Ashkenazi, A., Pai, R. C., Fong, S., Leung, S., Lawrence, D. A., Marsters, S. A., Blackie, C., Chang, L., McMurtrey, A. E., Hebert, A., DeForge, L., Koumenis, I. L., Lewis, D., Harris, L., Bussiere, J., Koeppen, H., Shahrokh, Z., and Schwall, R. H. Safety and antitumor activity of recombinant soluble Apo2 ligand. J Clin Invest, *104:* 155-162, 1999.
4. Sheridan, J. P., Marsters, S. A., Pitti, R. M., Gurney, A., Skubatch, M., Baldwin, D., Ramakrishnan, L., Gray, C. L., Baker, K., Wood, W. I., Goddard, A. D., Godowski, P., and Ashkenazi, A. Control of TRAIL-induced apoptosis by a family of signaling and decoy receptors. Science, *277:* 818-821, 1997.
5. Pan, G., O'Rourke, K., Chinnaiyan, A. M., Gentz, R., Ebner, R., Ni, J., and Dixit, V. M. The receptor for the cytotoxic ligand TRAIL. Science, *276:* 111-113, 1997.
6. Pan, G., Ni, J., Wei, Y. F., Yu, G., Gentz, R., and Dixit, V. M. An antagonist decoy receptor and a death domain-containing receptor for TRAIL. Science, *277:* 815-818, 1997.
7. Schneider, P., Bodmer, J. L., Thome, M., Hofmann, K., Holler, N., and Tschopp, J. Characterization of two receptors for TRAIL. FEBS Lett, *416:* 329-334, 1997.
8. Kischkel, F. C., Hellbardt, S., Behrmann, I., Germer, M., Pawlita, M., Krammer, P. H., and Peter, M. E. Cytotoxicity-dependent APO-1 (Fas/CD95)-associated proteins form a death-inducing signaling complex (DISC) with the receptor. Embo J, *14:* 5579-5588, 1995.
9. Wang, S. and El-Deiry, W. S. TRAIL and apoptosis induction by TNF-family death receptors. Oncogene, *22:* 8628-8633, 2003.
10. Kischkel, F. C., Lawrence, D. A., Chuntharapai, A., Schow, P., Kim, K. J., and Ashkenazi, A. Apo2L/TRAIL-dependent recruitment of endogenous FADD and caspase-8 to death receptors 4 and 5. Immunity, *12:* 611-620, 2000.
11. Sprick, M. R., Weigand, M. A., Rieser, E., Rauch, C. T., Juo, P., Blenis, J., Krammer, P. H., and Walczak, H. FADD/MORT1 and caspase-8 are recruited to TRAIL receptors 1 and 2 and are essential for apoptosis mediated by TRAIL receptor 2. Immunity, *12:* 599-609, 2000.
12. Bodmer, J. L., Holler, N., Reynard, S., Vinciguerra, P., Schneider, P., Juo, P., Blenis, J., and Tschopp, J. TRAIL receptor-2 signals apoptosis through FADD and caspase-8. Nat Cell Biol, *2:* 241-243, 2000.
13. Kelley, S. K. and Ashkenazi, A. Targeting death receptors in cancer with Apo2L/TRAIL. Curr Opin Pharmacol, *4:* 333-339, 2004.
14. Pickart, C. M. Back to the future with ubiquitin. Cell, *116:* 181-190, 2004.
15. Goldberg, A. L., Stein, R., and Adams, J. New insights into proteasome function: from archaebacteria to drug development. Chem Biol, *2:* 503-508, 1995.
16. Rock, K. L., Gramm, C., Rothstein, L., Clark, K., Stein, R., Dick, L., Hwang, D., and Goldberg, A. L. Inhibitors of the proteasome block the degradation of most cell proteins and the generation of peptides presented on MHC class I molecules. Cell, *78:* 761-771, 1994.
17. Adams, J., Palombella, V. J., and Elliott, P. J. Proteasome inhibition: a new strategy in cancer treatment. Invest New Drugs, *18:* 109-121, 2000.
18. Adams, J. Proteasome inhibition in cancer: development of PS-341. Semin Oncol, *28:* 613-619, 2001.
19. Adams, J., Palombella, V. J., Sausville, E. A., Johnson, J., Destree, A., Lazarus, D. D., Maas, J., Pien, C. S., Prakash, S., and Elliott, P. J. Proteasome inhibitors: a novel class of potent and effective antitumor agents. Cancer Res, *59:* 2615-2622, 1999.
20. Shah, S. A., Potter, M. W., McDade, T. P., Ricciardi, R., Perugini, R. A., Elliott, P. J., Adams, J., and Callery, M. P. 26S proteasome inhibition induces apoptosis and limits growth of human pancreatic cancer. J Cell Biochem, *82:* 110-122, 2001.

21. Bold, R. J., Virudachalam, S., and McConkey, D. J. Chemosensitization of pancreatic cancer by inhibition of the 26S proteasome. J Surg Res, *100:* 11-17, 2001.
22. Sunwoo, J. B., Chen, Z., Dong, G., Yeh, N., Crowl Bancroft, C., Sausville, E., Adams, J., Elliott, P., and Van Waes, C. Novel proteasome inhibitor PS-341 inhibits activation of nuclear factor-kappa B, cell survival, tumor growth, and angiogenesis in squamous cell carcinoma. Clin Cancer Res, *7:* 1419-1428, 2001.
23. Nawrocki, S. T., Sweeney-Gotsch, B., Takamori, R., and McConkey, D. J. The proteasome inhibitor bortezomib enhances the activity of docetaxel in orthotopic human pancreatic tumor xenografts. Mol Cancer Ther, *3:* 59-70, 2004.
24. Pettaway, C. A., Pathak, S., Greene, G., Ramirez, E., Wilson, M. R., Killion, J. J., and Fidler, I. J. Selection of highly metastatic variants of different human prostatic carcinomas using orthotopic implantation in nude mice. Clin Cancer Res, *2:* 1627-1636, 1996.
25. Dinney, C. P., Fishbeck, R., Singh, R. K., Eve, B., Pathak, S., Brown, N., Xie, B., Fan, D., Bucana, C. D., and Fidler, I. J. Isolation and characterization of metastatic variants from human transitional cell carcinoma passaged by orthotopic implantation in athymic nude mice. J Urol, *154:* 1532-1538, 1995.
26. Nicoletti, I., Migliorati, G., Pagliacci, M. C., Grignani, F., and Riccardi, C. A rapid and simple method for measuring thymocyte apoptosis by propidium iodide staining and flow cytometry. J Immunol Methods, *139:* 271-279, 1991.
27. Koopman, G., Reutelingsperger, C. P., Kuijten, G. A., Keehnen, R. M., Pals, S. T., and van Oers, M. H. Annexin V for flow cytometric detection of phosphatidylserine expression on B cells undergoing apoptosis. Blood, *84:* 1415-1420, 1994.
28. Jeremias, I., Kupatt, C., Baumann, B., Herr, I., Wirth, T., and Debatin, K. M. Inhibition of nuclear factor kappaB activation attenuates apoptosis resistance in lymphoid cells. Blood, *91:* 4624-4631, 1998.
29. Keane, M. M., Rubinstein, Y., Cuello, M., Ettenberg, S. A., Banerjee, P., Nau, M. M., and Lipkowitz, S. Inhibition of NF-kappaB activity enhances TRAIL mediated apoptosis in breast cancer cell lines. Breast Cancer Res Treat, *64:* 211-219, 2000.
30. Nawrocki, S. T., Bruns, C. J., Harbison, M. T., Bold, R. J., Gotsch, B. S., Abbruzzese, J. L., Elliott, P., Adams, J., and McConkey, D. J. Effects of the proteasome inhibitor PS-341 on apoptosis and angiogenesis in orthotopic human pancreatic tumor xenografts. Mol Cancer Ther, *1:* 1243-1253, 2002.
31. Hideshima, T., Chauhan, D., Richardson, P., Mitsiades, C., Mitsiades, N., Hayashi, T., Munshi, N., Dang, L., Castro, A., Palombella, V., Adams, J., and Anderson, K. C. NF-kappa B as a therapeutic target in multiple myeloma. J Biol Chem, *277:* 16639-16647, 2002.
32. Ashkenazi, A. and Dixit, V. M. Apoptosis control by death and decoy receptors. Curr Opin Cell Biol, *11:* 255-260, 1999.
33. Kamat, A. M., Karashima, T., Davis, D. W., Lashinger, L., Bar-Eli, M., Millikan, R., Shen, Y., Dinney, C. P., and McConkey, D. J. The proteasome inhibitor bortezomib synergizes with gemcitabine to block the growth of human 253JB-V bladder tumors in vivo. Mol Cancer Ther, *3:* 279-290, 2004.
34. Williams, S., Pettaway, C., Song, R., Papandreou, C., Logothetis, C., and McConkey, D. J. Differential effects of the proteasome inhibitor bortezomib on apoptosis and angiogenesis in human prostate tumor xenografts. Mol Cancer Ther, *2:* 835-843, 2003.
35. An, W. G., Hwang, S. G., Trepel, J. B., and Blagosklonny, M. V. Protease inhibitor-induced apoptosis: accumulation of wt p53, p21WAF1/CIP1, and induction of apoptosis are independent markers of proteasome inhibition. Leukemia, *14:* 1276-1283, 2000.
36. Blagosklonny, M. V. Flavopiridol, an inhibitor of transcription: implications, problems and solutions. Cell Cycle, *3:* 1537-1542, 2004.
37. Demidenko, Z. N. and Blagosklonny, M. V. Flavopiridol induces p53 via initial inhibition of Mdm2 and p21 and, independently of p53, sensitizes apoptosis-reluctant cells to tumor necrosis factor. Cancer Res, *64:* 3653-3660, 2004.
38. Orlowski, R. Z. and Baldwin, A. S., Jr. NF-kappaB as a therapeutic target in cancer. Trends Mol Med, *8:* 385-389, 2002.

39. Kim, E. H., Kim, S. U., Shin, D. Y., and Choi, K. S. Roscovitine sensitizes glioma cells to TRAIL-mediated apoptosis by downregulation of survivin and XIAP. Oncogene, *23:* 446-456, 2004.
40. Kim, D. M., Koo, S. Y., Jeon, K., Kim, M. H., Lee, J., Hong, C. Y., and Jeong, S. Rapid induction of apoptosis by combination of flavopiridol and tumor necrosis factor (TNF)-alpha or TNF-related apoptosis-inducing ligand in human cancer cell lines. Cancer Res, *63:* 621-626, 2003.
41. Taniai, M., Grambihler, A., Higuchi, H., Werneburg, N., Bronk, S. F., Farrugia, D. J., Kaufmann, S. H., and Gores, G. J. Mcl-1 mediates tumor necrosis factor-related apoptosis-inducing ligand resistance in human cholangiocarcinoma cells. Cancer Res, *64:* 3517-3524, 2004.
42. Rosato, R. R., Dai, Y., Almenara, J. A., Maggio, S. C., and Grant, S. Potent antileukemic interactions between flavopiridol and TRAIL/Apo2L involve flavopiridol-mediated XIAP downregulation. Leukemia, 2004.
43. Jin, Z., Dicker, D. T., and El-Deiry, W. S. Enhanced sensitivity of G1 arrested human cancer cells suggests a novel therapeutic strategy using a combination of simvastatin and TRAIL. Cell Cycle, *1:* 82-89, 2002.
44. Wang, S. and El-Deiry, W. S. Requirement of p53 targets in chemosensitization of colonic carcinoma to death ligand therapy. Proc Natl Acad Sci U S A, *100:* 15095-15100, 2003.
45. Fulda, S. and Debatin, K. M. Sensitization for tumor necrosis factor-related apoptosis-inducing ligand-induced apoptosis by the chemopreventive agent resveratrol. Cancer Res, *64:* 337-346, 2004.
46. Rosato, R. R., Almenara, J. A., Dai, Y., and Grant, S. Simultaneous activation of the intrinsic and extrinsic pathways by histone deacetylase (HDAC) inhibitors and tumor necrosis factor-related apoptosis-inducing ligand (TRAIL) synergistically induces mitochondrial damage and apoptosis in human leukemia cells. Mol Cancer Ther, *2:* 1273-1284, 2003.
47. Nakata, S., Yoshida, T., Horinaka, M., Shiraishi, T., Wakada, M., and Sakai, T. Histone deacetylase inhibitors upregulate death receptor 5/TRAIL-R2 and sensitize apoptosis induced by TRAIL/APO2-L in human malignant tumor cells. Oncogene, *23:* 6261-6271, 2004.
48. Johnson, T. R., Stone, K., Nikrad, M., Yeh, T., Zong, W. X., Thompson, C. B., Nesterov, A., and Kraft, A. S. The proteasome inhibitor PS-341 overcomes TRAIL resistance in Bax and caspase 9-negative or Bcl-xL overexpressing cells. Oncogene, *22:* 4953-4963, 2003.
49. Sayers, T. J., Brooks, A. D., Koh, C. Y., Ma, W., Seki, N., Raziuddin, A., Blazar, B. R., Zhang, X., Elliott, P. J., and Murphy, W. J. The proteasome inhibitor PS-341 sensitizes neoplastic cells to TRAIL-mediated apoptosis by reducing levels of c-FLIP. Blood, *102:* 303-310, 2003.
50. Shimada, K., Matsuyoshi, S., Nakamura, M., Ishida, E., Kishi, M., and Konishi, N. Phosphorylation of FADD is critical for sensitivity to anticancer drug-induced apoptosis. Carcinogenesis, *25:* 1089-1097, 2004.
51. Scaffidi, C., Volkland, J., Blomberg, I., Hoffmann, I., Krammer, P. H., and Peter, M. E. Phosphorylation of FADD/ MORT1 at serine 194 and association with a 70-kDa cell cycle-regulated protein kinase. J Immunol, *164:* 1236-1242, 2000.
52. Alappat, E. C., Volkland, J., and Peter, M. E. Cell cycle effects by C-FADD depend on its C-terminal phosphorylation site. J Biol Chem, *278:* 41585-41588, 2003.
53. Harrington, E. A., Fanidi, A., and Evan, G. I. Oncogenes and cell death. Curr Opin Genet Dev, *4:* 120-129, 1994.
54. Owa, T., Yoshino, H., Yoshimatsu, K., and Nagasu, T. Cell cycle regulation in the G1 phase: a promising target for the development of new chemotherapeutic anticancer agents. Curr Med Chem, *8:* 1487-1503, 2001.

FIGURE LEGENDS

Figure 1. Effects of bortezomib on TRAIL-induced apoptosis. A. Effects on DNA fragmentation. Cells were incubated in the absence or presence of 10 ng/ml recombinant human TRAIL with or without 100 nM bortezomib (BZ) for 24 h and DNA fragmentation was quantified by PI/FACS as described in Materials and Methods. Mean ± S.E.M., n = 3, *$p < 0.01$. B. Effects on phosphatidylserine exposure. Cells were incubated for 24 h as described above, and externalization of PS was quantified by immunofluorescence annexin-V staining and FACS analysis as described in Materials and Methods. Mean ± S.E.M., n = 3, *$p < 0.01$. C. Effects of the IKK inhibitor, PS-1145, on TRAIL-induced apoptosis. Cells were incubated for 24 h in the absence or presence of 10 ng/ml recombinant human TRAIL with or without 50 μM PS-1145 and DNA fragmentation was measured by PI/FACS as described in Materials and Methods. Mean ± S.E.M., n = 3.

Figure 2. Characterization of the effects of bortezomib on sentinel steps within the TRAIL cell death pathway. A. Kinetics of DNA fragmentation. 253J B-V or LNCaP-Pro5 cells were incubated in the absence or presence of 10 ng/ml TRAIL, 100 nM bortezomib (BZ), or both for the times indicated and DNA fragmentation was measured by PI/FACS as described in Materials and Methods. Mean ± S.E.M., n = 3. B. Effects on procaspase-8 processing. 253J B-V or LNCaP-Pro5 cells were incubated with TRAIL with or without bortezomib (BZ) for the times indicated and proteolytic processing (activation) of procaspase-8 was analyzed by immunoblotting. Note that the appearance of the completely processed, active p18 caspase-8 fragment appears within 30 min in

both cell lines. Results are representative of those obtained in 3 separate experiments. C. Effects on cytochrome c release (top panels) and Bid cleavage (bottom panels). Cells were incubated with 10 ng/ml TRAIL with or without 100 nM bortezomib for the times indicated. Cytochrome c release was measured in cytosolic extracts and the disappearance of the intact form of Bid was measured in total cell extracts by immunoblotting as described in Materials and Methods. In the cytochrome c experiment, the *top panel* displays the cytochrome c present in the cytosolic fraction, and the *bottom panel* displays the cytochrome c present in the membrane fraction. Note that the TRAIL plus bortezomib combination induces cytochrome c release by 4 h in both cell types. Results are representative of those obtained in 3 separate experiments. D. Effects on caspase-3 activation. 253J B-V or LNCaP-Pro5 cells were incubated with 10 ng/ml TRAIL in the absence or presence of 100 nM bortezomib for the times indicated. Caspase-3 proteolytic activity was quantified in cytosolic extracts using a DEVD-AFC fluorigenic peptide as described in Materials and Methods (top panel). Mean ± S.D., Proteolytic processing of procaspase-3 was also measured in total cell extracts by immunoblotting. Percentages of hypodiploid cells were measured in parallel and are indicated below each immunoblot. Note the appearance of active p20/p17 fragments by 4 h in cells treated with TRAIL plus bortezomib. Results are representative of those obtained in 3 separate experiments.

Figure 3. Effects of bortezomib on cdk activity. A. Effects of bortezomib on p21 accumulation in LNCaP-Pro5 cells. Cells were incubated in the absence or presence of 100 nM bortezomib, 10 ng/ml TRAIL, or both, and p21 expression was measured in total

cell extracts by immunoblotting (upper panel). Expression of actin was measured in parallel as a loading control. Results are representative of those obtained in 3 separate experiments. B. Effects of bortezomib and roscovitine on cdk2 activity. LNCaP-Pro5 cells were incubated for 16 h in the presence of the indicated concentrations of either agent and cdk2 kinase activity was measured in immunoprecipitates as described in Materials and Methods. Expression of cdk2 protein was quantified in parallel by immunoblotting and served as a loading control. Relative kinase activities were quantified in each condition by densitometry and standardized to control values (indicated below the immunoblot). Results are representative of those obtained in 3 separate experiments. C. Effects of roscovitine on TRAIL-induced DNA fragmentation. Cells were incubated with 10 ng/ml TRAIL with or without 25 μM roscovitine for 16 h and DNA fragmentation was quantified by PI/FACS. Mean ± S.E.M., n = 3.

Figure 4. Accumulation of p21 is required for bortezomib-mediated TRAIL sensitization. A. Effects of p21 silencing on DNA fragmentation. Cells were transiently transfected with an siRNA construct specific for p21 or a non-specific control construct for 48 h. Cells were then incubated for 8 h with 100 nM bortezomib, 10 ng/ml TRAIL, or both agents, and DNA fragmentation was measured by PI/FACS. Mean ± S.E.M., n = 3, *$p < 0.01$. In the *bottom panel*, the effects of p21 silencing on protein expression were measured by immunoblotting. Results are representative of those obtained in 3 separate experiments. B. Effects of p27 silencing on DNA fragmentation. Cells were transiently transfected with an siRNA construct specific for p27 or a non-specific control construct for 48 h. Cells were then incubated for 8 h with 100 nM bortezomib, 10 ng/ml TRAIL,

or both agents, and DNA fragmentation was measured by PI/FACS. Mean ± S.E.M., n = 3. In the *bottom panel*, the effects of p27 silencing on protein expression were measured by immunoblotting. Results are representative of those obtained in 3 separate experiments. C. Effects of p21 silencing on procaspase-8 and –3 activation. Cells were transfected with the p21-specific siRNA construct or a control construct for 48 h. Cells were then incubated for 8 h with 100 nM bortezomib, 10 ng/ml TRAIL, or both agents for 8 h, and procaspase-8 and –3 were visualized by immunoblotting. Actin served as a control for protein loading. *Arrows* indicate mature large subunits of caspase-8 and –3. Note that these mature forms are absent in the p21-silenced cells.

Fig. 1A.

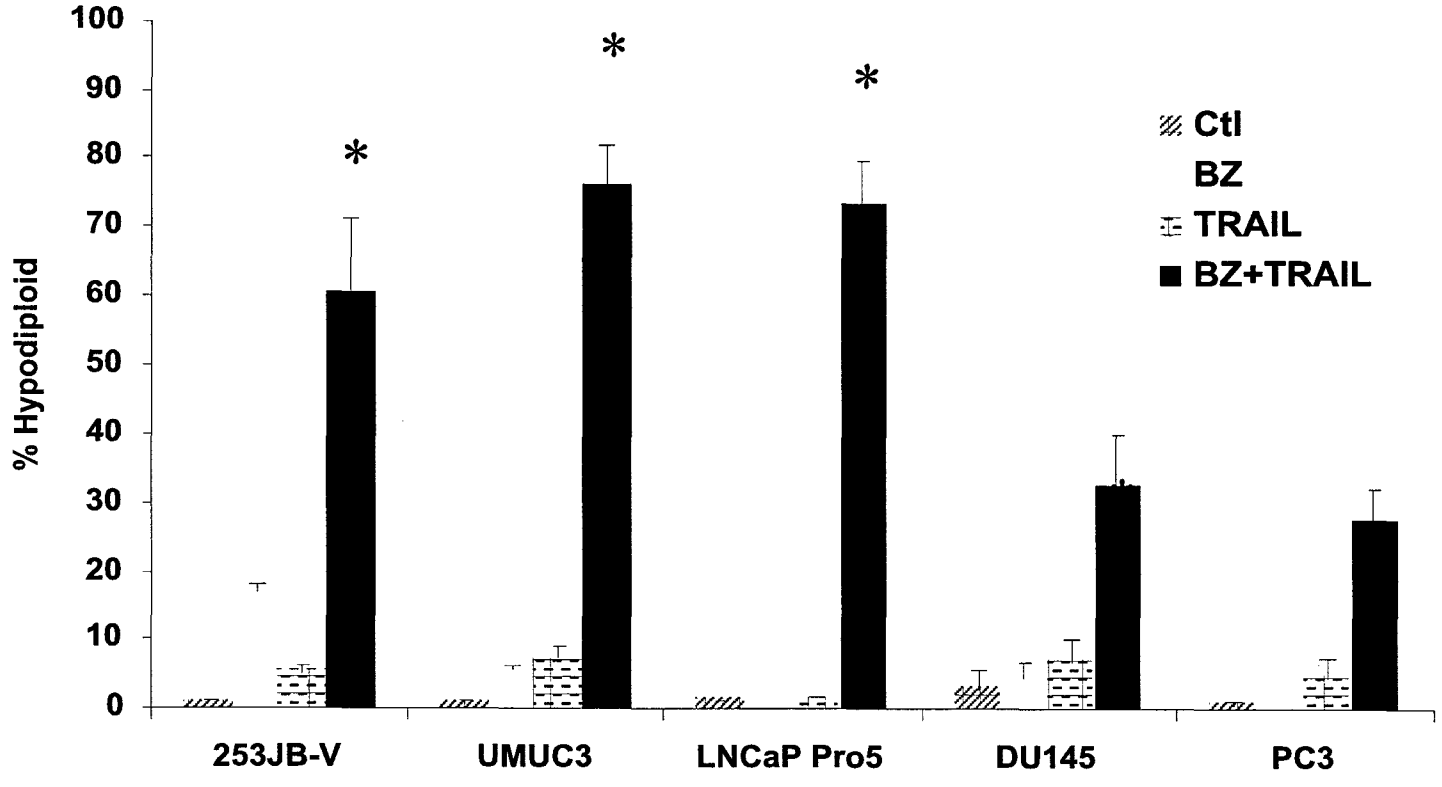
100
90
80
70
60
50
40
30
20
10
0
% Hypodiploid
*
*
*
Ctl
BZ
TRAIL
BZ+TRAIL
253JB-V
UMUC3
LNCaP Pro5
DU145
PC3

Fig. 1B.

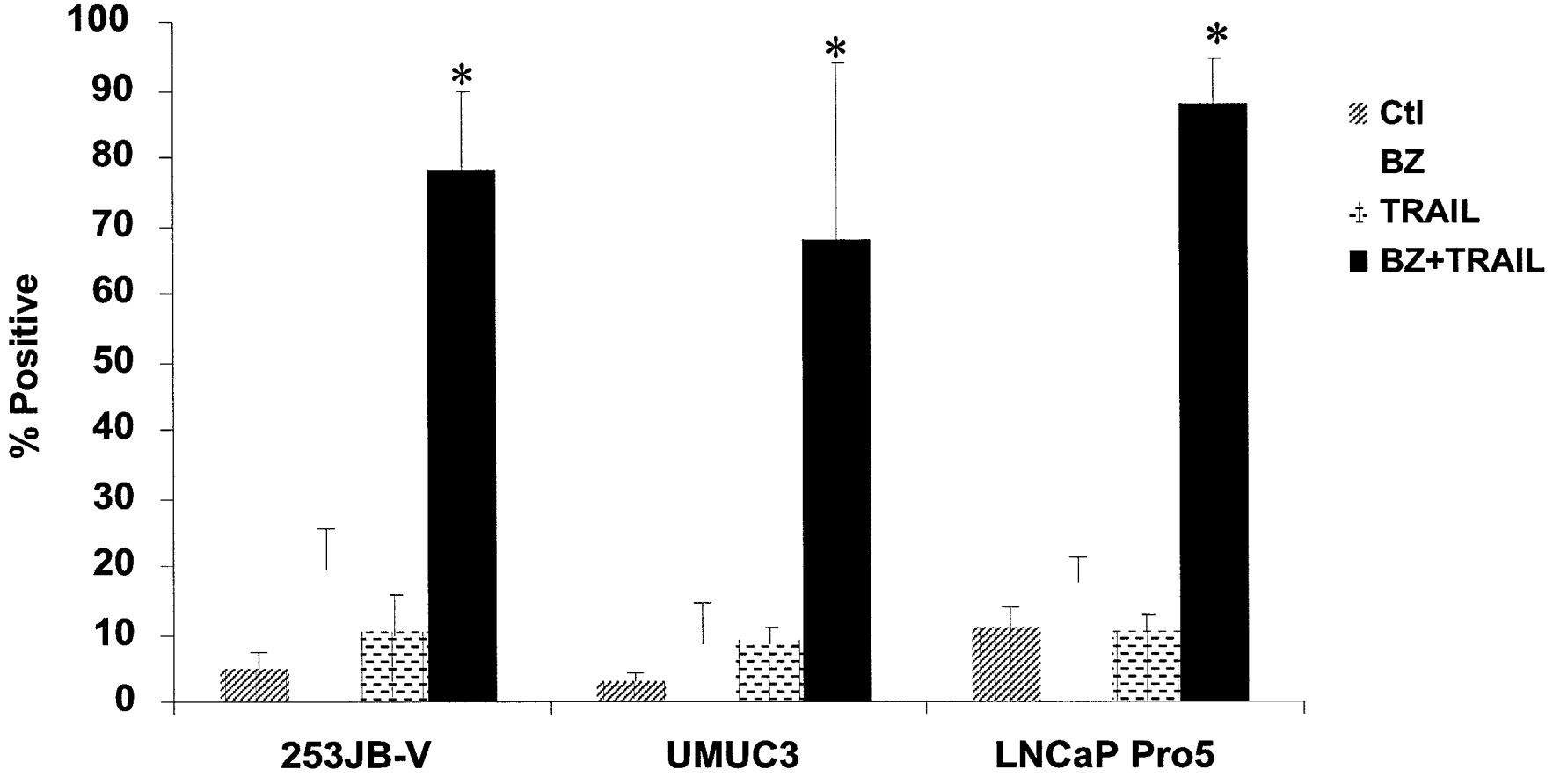
100
90
80
70
60
50
40
30
20
10
0
% Positive
*
*
*
253JB-V
UMUC3
LNCaP Pro5
Ctl
BZ
TRAIL
BZ+TRAIL

Fig. 1C.

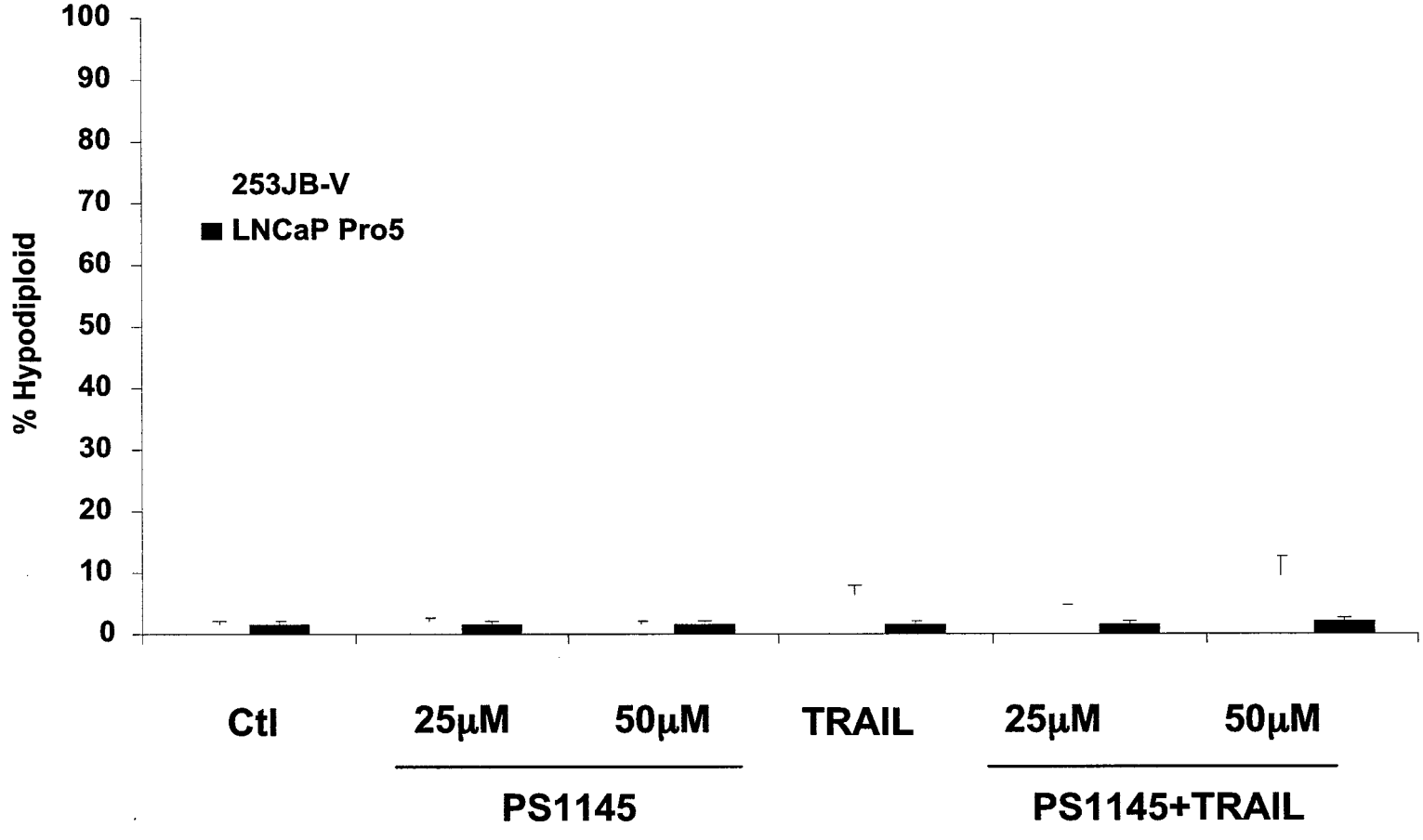
100
90
80
70
60
50
40
30
20
10
0
% Hypodiploid
253JB-V
LNCaP Pro5
Ctl
25μM
50μM
TRAIL
25μM
50μM
PS1145
PS1145+TRAIL

Fig. 2A.

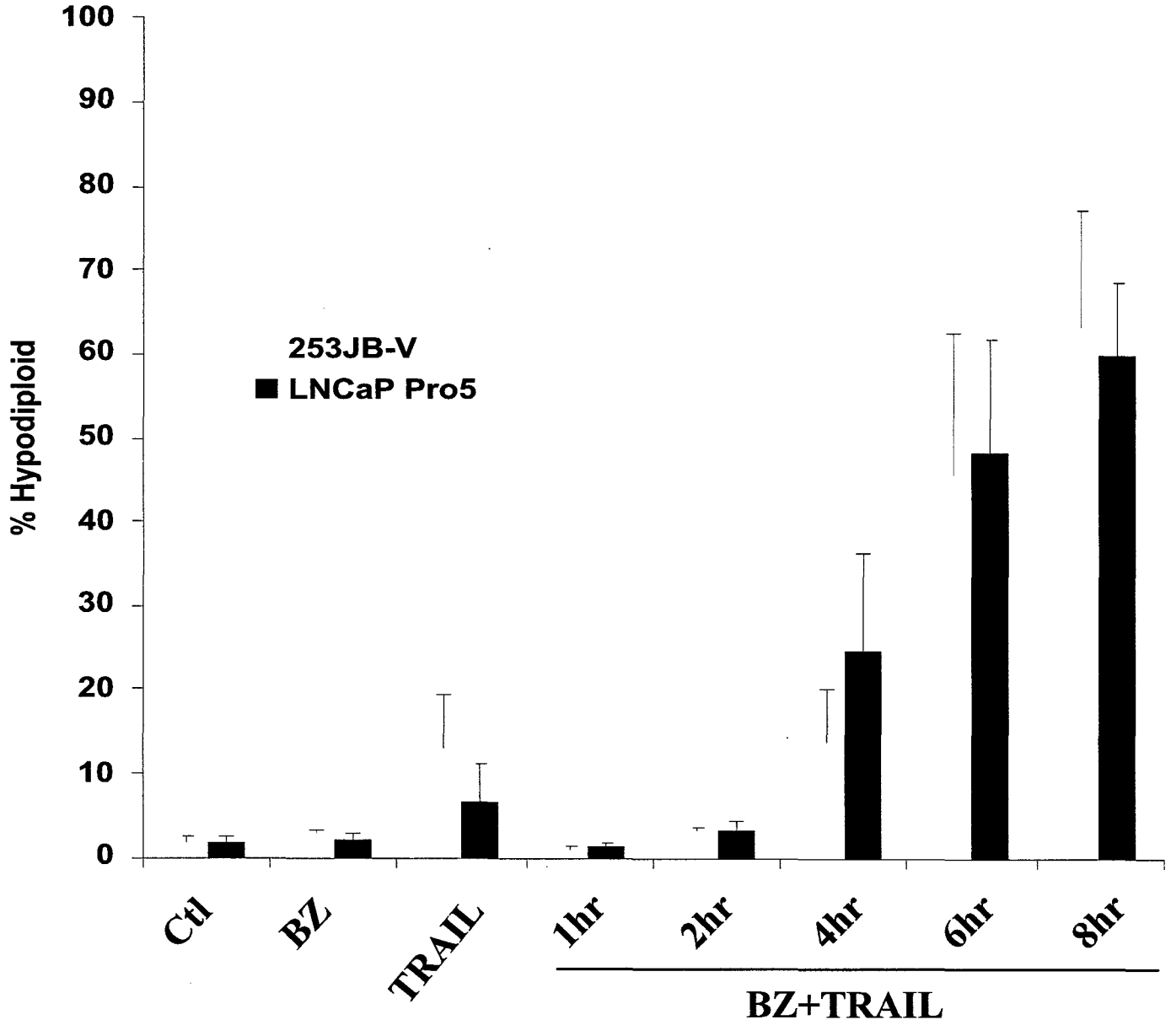
100
90
80
70
60
50
40
30
20
10
0
% Hypodiploid
253JB-V
LNCaP Pro5
Ctl
BZ
TRAIL
1hr
2hr
4hr
6hr
8hr
BZ+TRAIL

Fig. 2B.

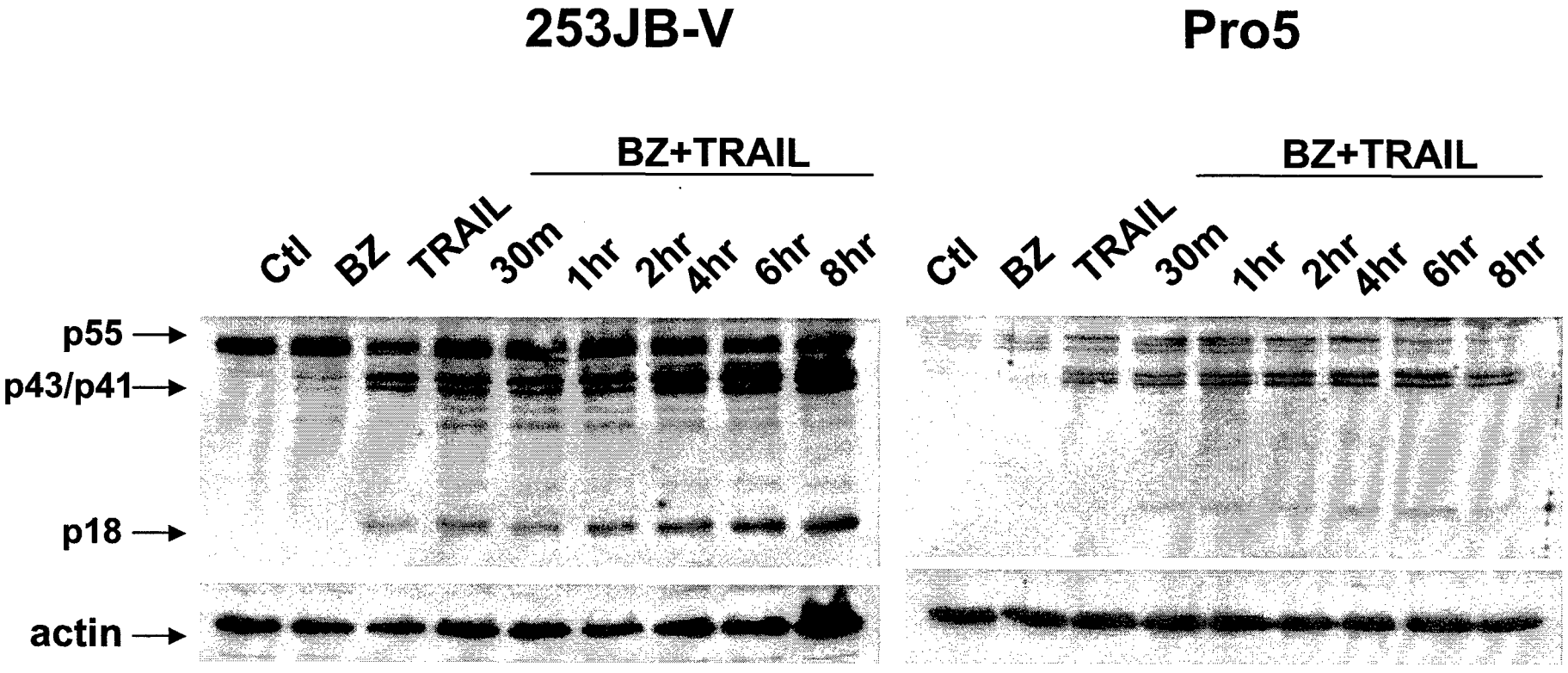
253JB-V
Pro5
BZ+TRAIL
BZ+TRAIL
Ctl
BZ
TRAIL
30m
1hr
2hr
4hr
6hr
8hr
Ctl
BZ
TRAIL
30m
1hr
2hr
4hr
6hr
8hr
p55
p43/p41
p18
actin

Fig. 2C.

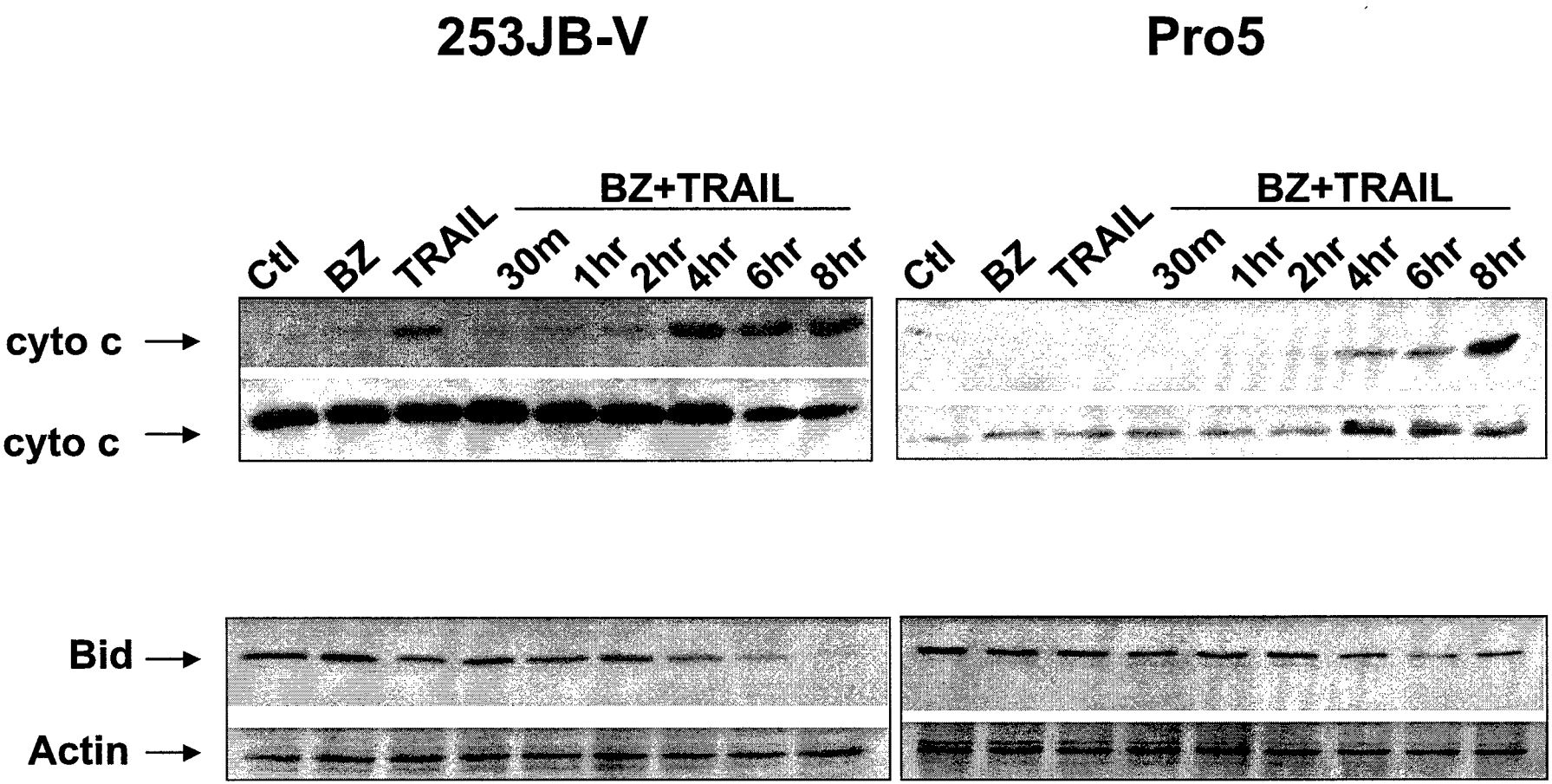
253JB-V
Pro5
BZ+TRAIL
BZ+TRAIL
Ctl
BZ
TRAIL
30m
1hr
2hr
4hr
6hr
8hr
Ctl
BZ
TRAIL
30m
1hr
2hr
4hr
6hr
8hr
cyto c
cyto c
Bid
Actin

Fig. 2D.

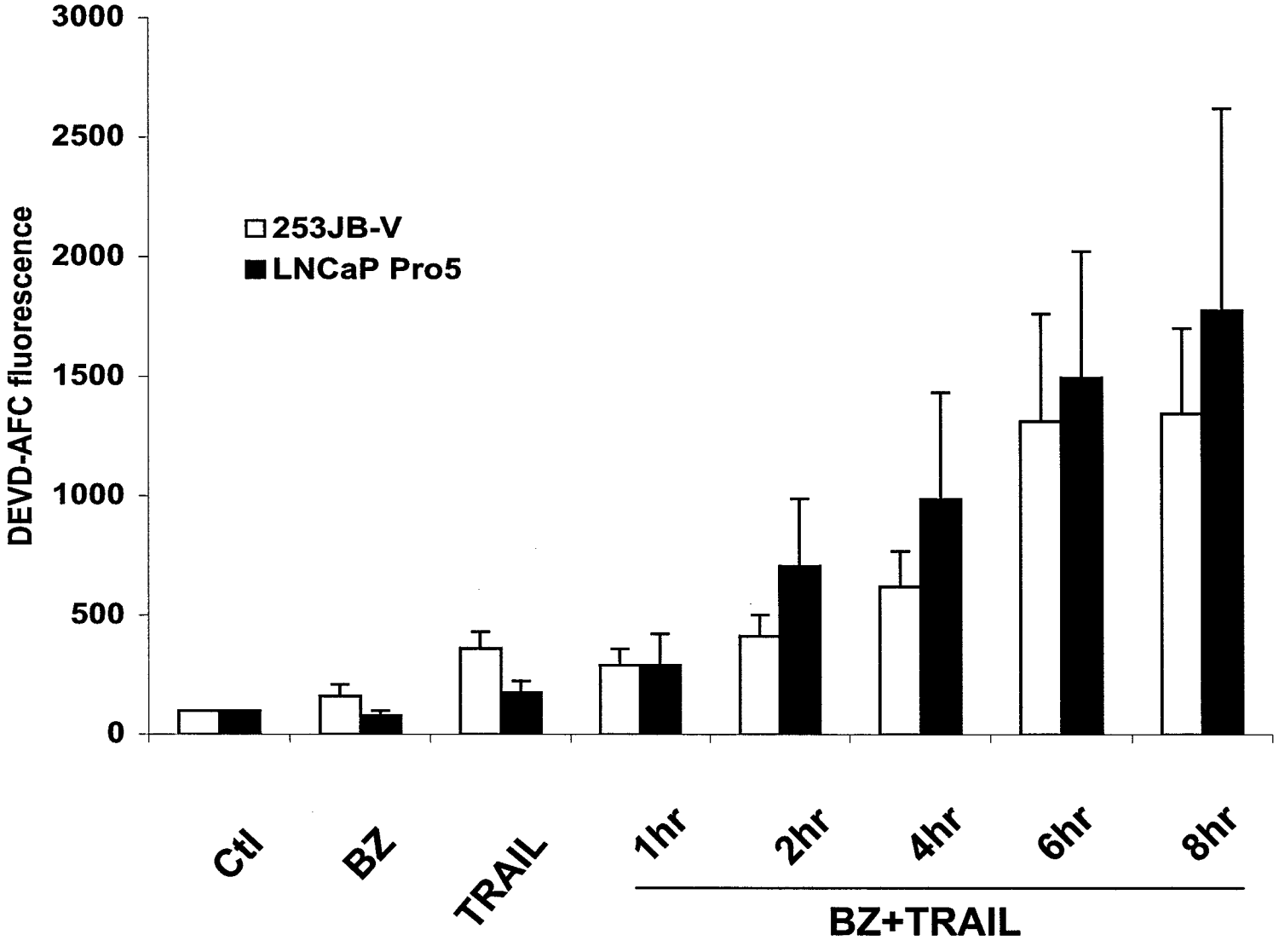
3000
2500
2000
1500
1000
500
0
DEVD-AFC fluorescence
253JB-V
LNCaP Pro5
Ctl
BZ
TRAIL
1hr
2hr
4hr
6hr
8hr
BZ+TRAIL

Fig. 2D.

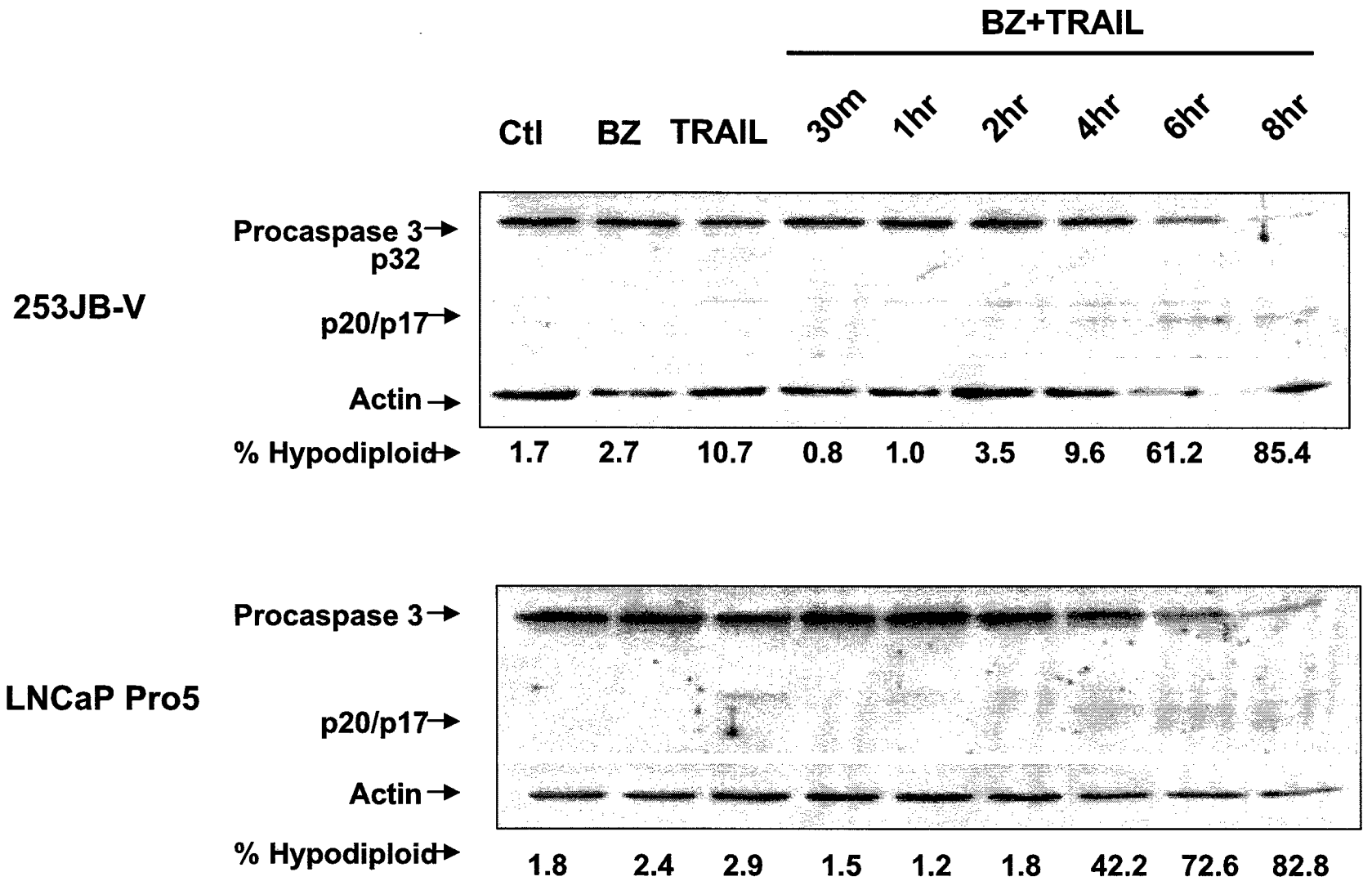
BZ+TRAIL
Ctl
BZ
TRAIL
30m
1hr
2hr
4hr
6hr
8hr
253JB-V
Procaspase 3
p32
p20/p17
Actin
% Hypodiploid
1.7
2.7
10.7
0.8
1.0
3.5
9.6
61.2
85.4
LNCaP Pro5
Procaspase 3
p20/p17
Actin
% Hypodiploid
1.8
2.4
2.9
1.5
1.2
1.8
42.2
72.6
82.8

Fig. 3A.

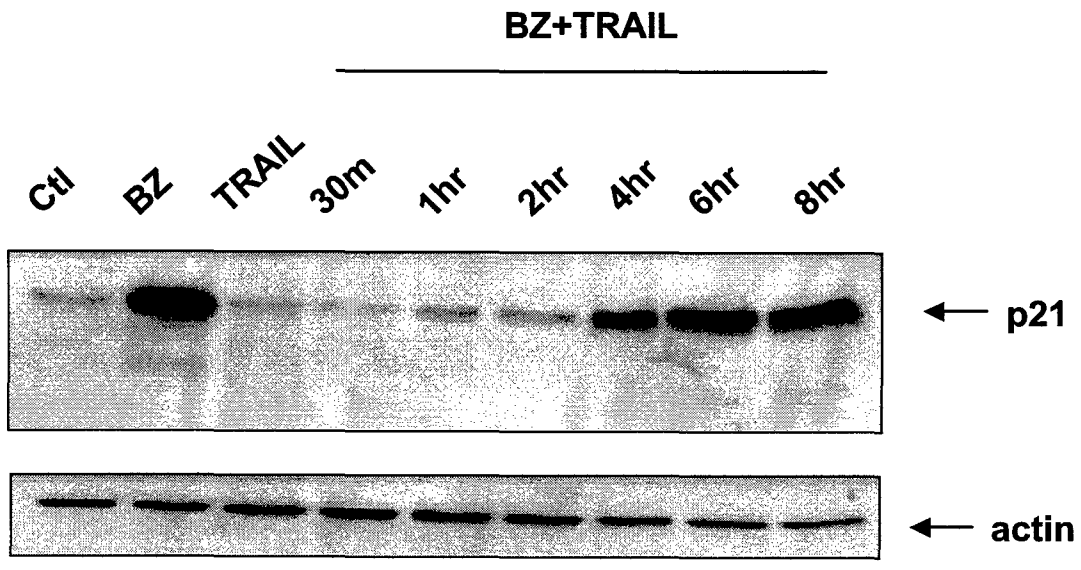

Fig. 3B.

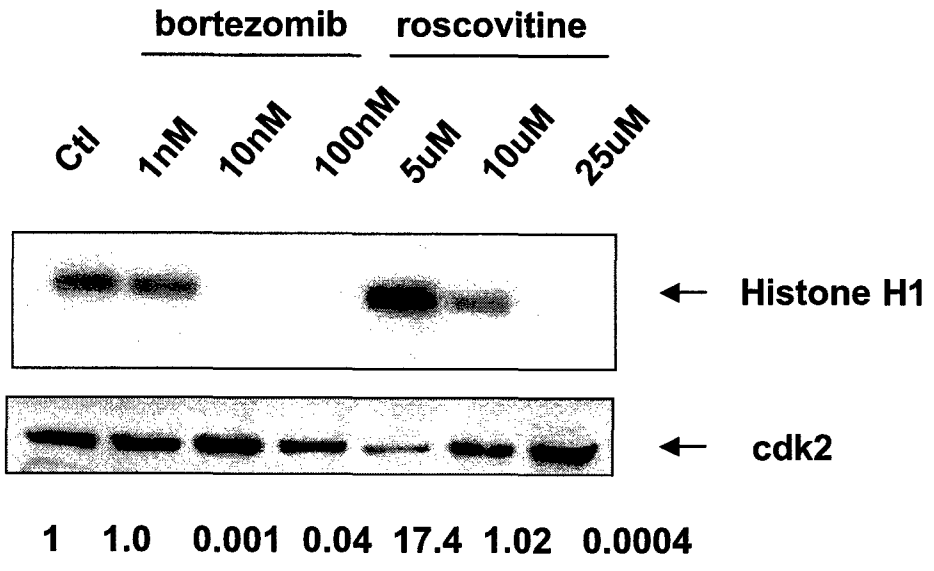
bortezomib
roscovitine
Ctl
1nM
10nM
100nM
5uM
10uM
25uM
Histone H1
cdk2
1
1.0
0.001
0.04
17.4
1.02
0.0004

Fig. 3C.

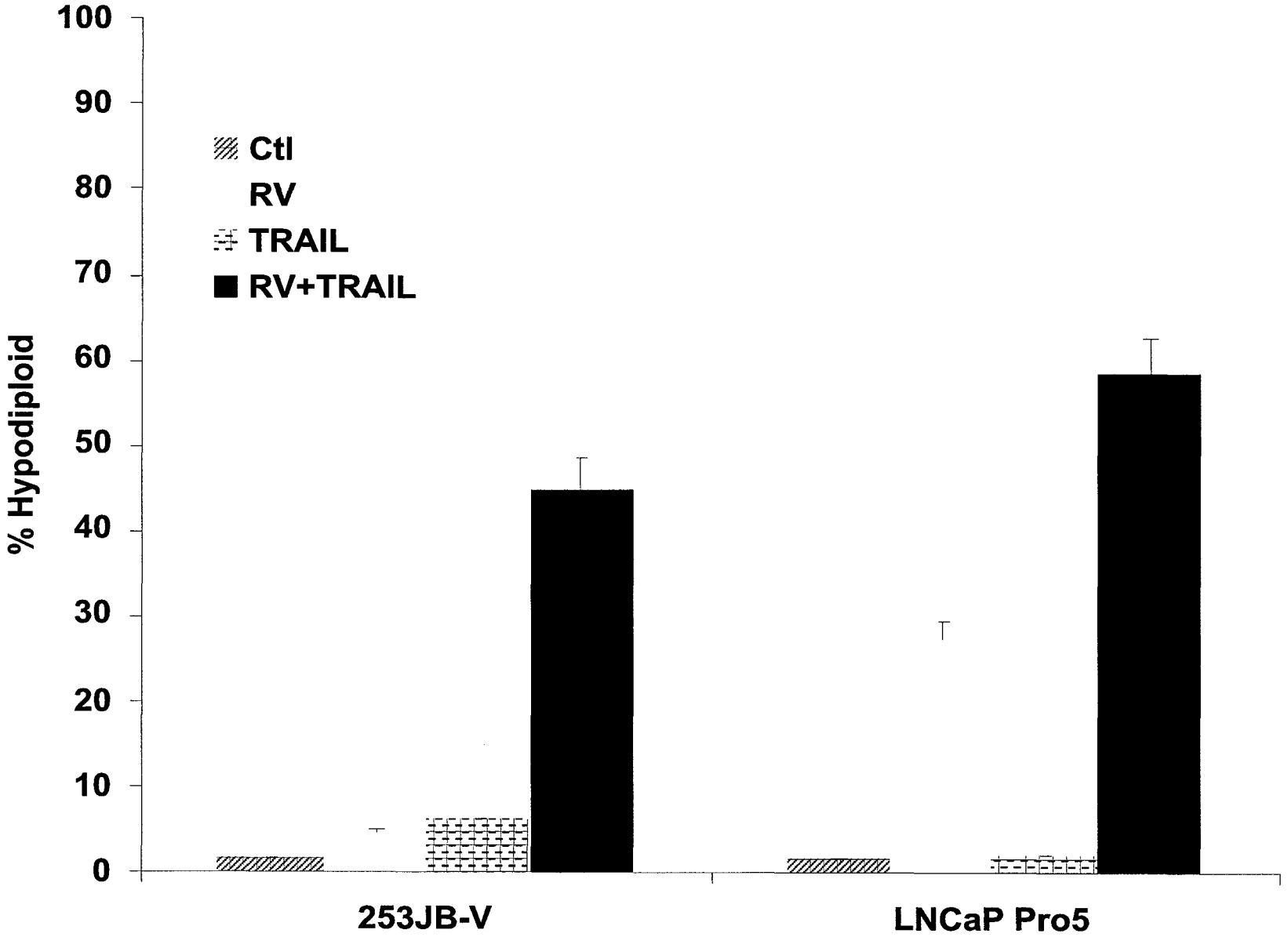
100
90
80
70
60
50
40
30
20
10
0
% Hypodiploid
Ctl
RV
TRAIL
RV+TRAIL
253JB-V
LNCaP Pro5

Fig. 4A

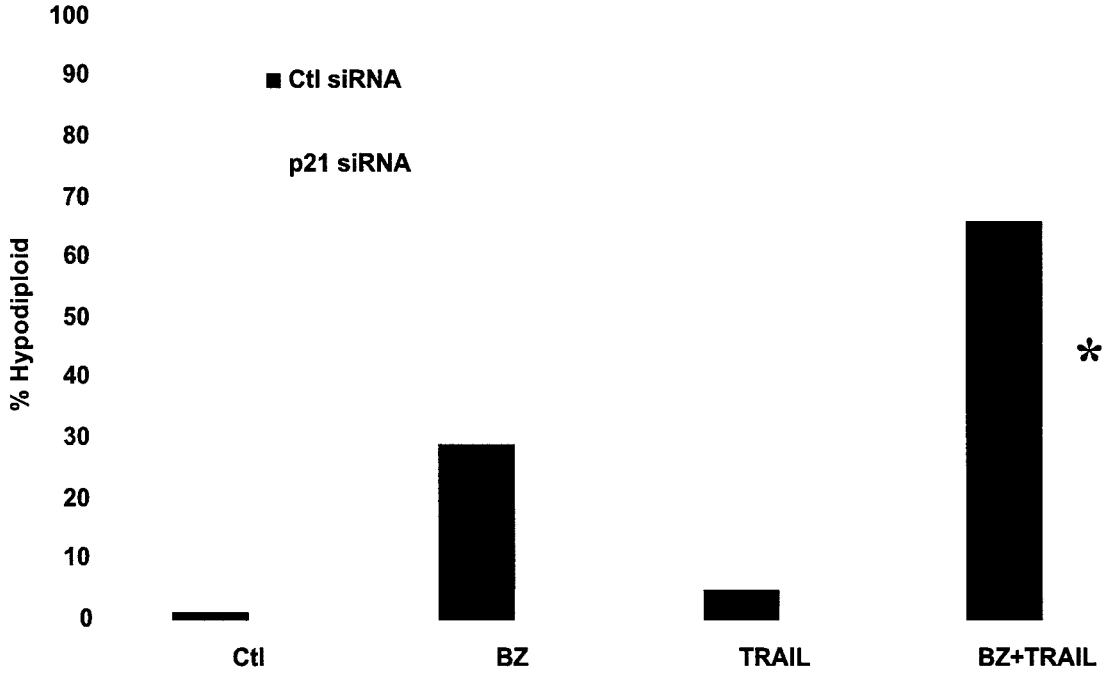
100
90
80
70
60
50
40
30
20
10
0
% Hypodiploid
Ctl siRNA
p21 siRNA
*
Ctl
BZ
TRAIL
BZ+TRAIL

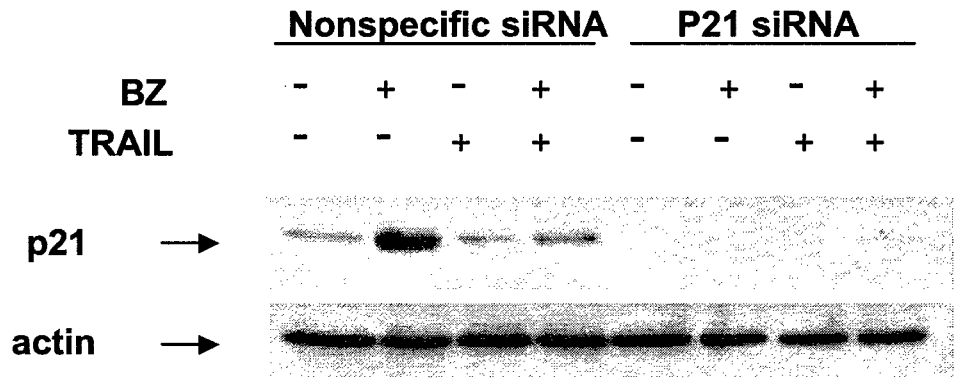
Nonspecific siRNA
P21 siRNA
BZ
TRAIL
- + - + - + - +
- - + + - - + +
p21
actin

Fig. 4B


80
70
60
50
40
30
20
10
0
% Hypodiploid
NS siRNA
p27 siRNA
Ctl
BZ
TRAIL
BZ+TRAIL

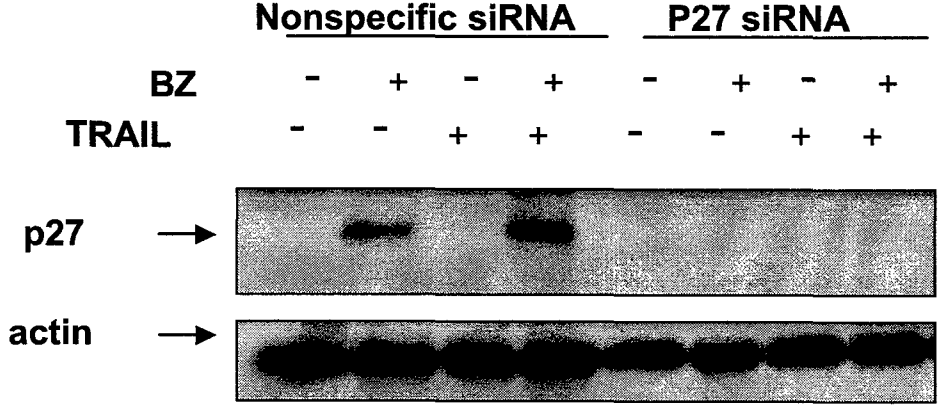
Nonspecific siRNA
P27 siRNA
BZ
TRAIL
p27
actin

Fig. 4C

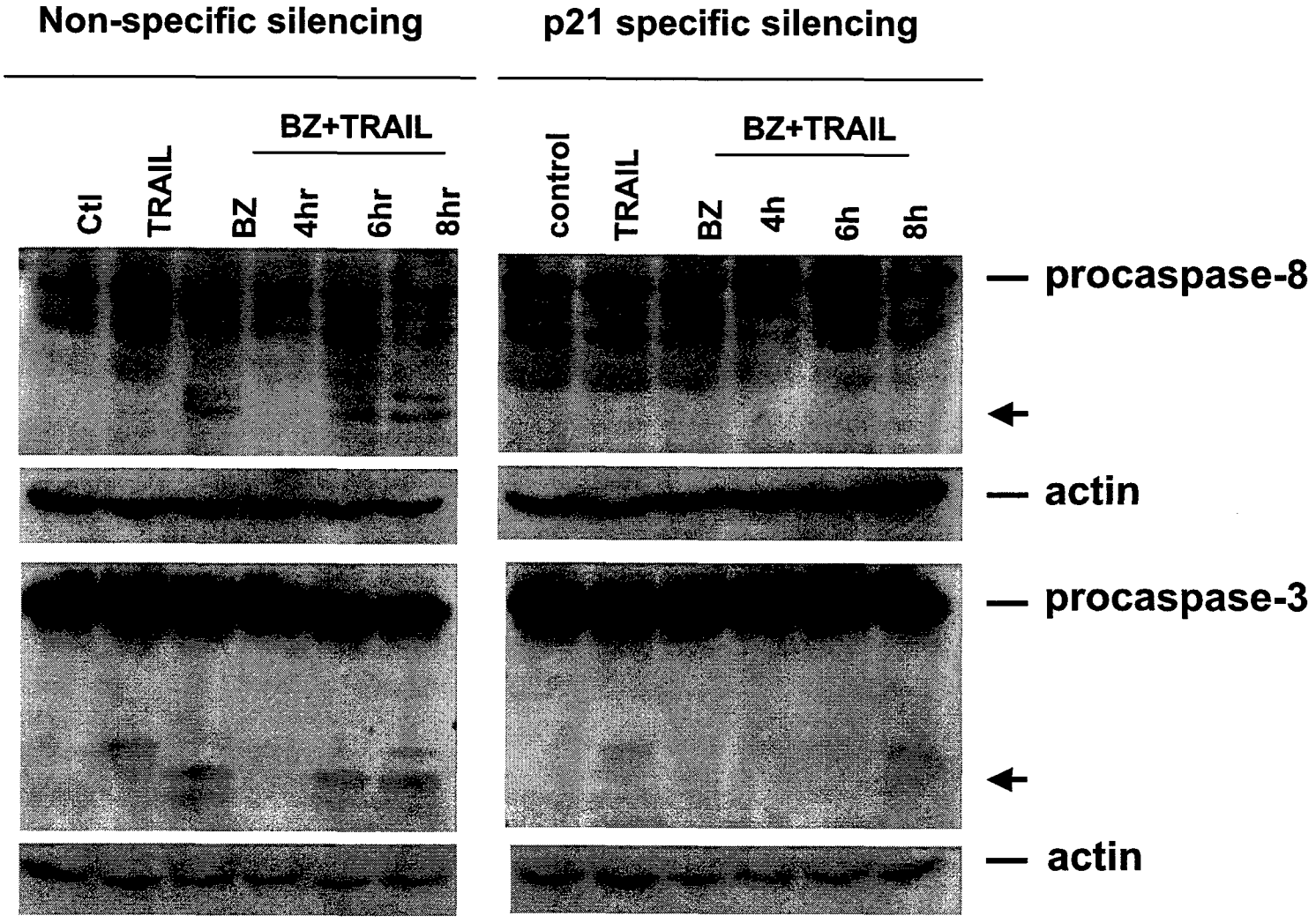
Non-specific silencing
p21 specific silencing
Ctl
TRAIL
BZ
BZ+TRAIL
4hr
6hr
8hr
control
TRAIL
BZ
BZ+TRAIL
4h
6h
8h
procaspase-8
actin
procaspase-3
actin